GEOMETRIC PHASES IN QUANTUM THEORY

Diplomarbeit
zur Erlangung des akademischen Grades einer
Magistra der Naturwissenschaften
an der
UNIVERSITÄT WIEN

eingereicht von
Katharina Durstberger

betreut von
Ao. Univ. Prof. Dr. Reinhold A. Bertlmann

Wien, im Jänner 2002

Science is built up with facts,
as a house is with stones.
But a collection of facts
is no more science
than a heap of stones
is a house.

H. Poincaré

DANKE ...

Contents

Chapter 1

Some introductory words

1.1 What do we mean by geometrical phases?

Geometrical phases arise due to a phenomenon which can be described roughly as "global change without local change". This can be easily shown with an example. Imagine a vector which marks a direction and put it on a 2-sphere, for example on the north pole and pointing in the direction of a certain meridian. Then you move the object keeping it always parallel to its initial direction down the meridian until you reach the equator and then move it parallel along the equator till another meridian which keeps an angle of θ with the original one. Then you move the vector back to the north pole along the new meridian again keeping it always parallel. When you reach the north pole you discover that the vector points not in the same direction as before. It has turned around an angle θ (see figure 1.1). This phenomenon which is called a holonomy[1] was already known to Gauss and can be described by the so called Hannay angles [37]. It arises due to parallel transport of a vector on a curved area, in this case on a S^2. We define parallelism as being parallel to a meridian but this cannot be done on the whole sphere. At least at one point you get in trouble with this definition. Sometimes this is called "to comb the hair on a sphere", which is not possible (see for instance [7]). The rotation of Foucault's pendulum can also be explained by such a holonomy (see [36]).

These are all classical examples where a geometrical angles arises although the system returns to its starting point. Nearly the same situation occurs in quantum physics. Here a system picks up a geometrical phase which can be identified with a Hannay angle in the classical limit.

It will be the aim of the present work to examine in detail the concept of the geometrical phases in quantum theory.

[1] In physics the word anholonomy is used to classify such phenomenons but in mathematics the word holonomy is used for it. So we should be a little bit careful using the words. In the following I will use the mathematical convention thus holonomy.

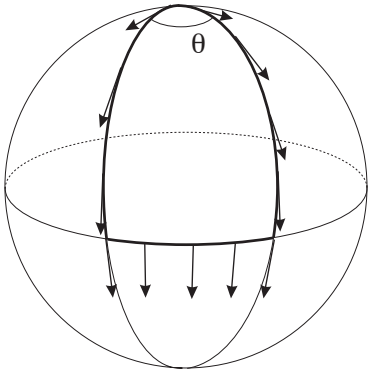

Figure 1.1: The holonomy due to the parallel transport of a vector.

1.2 A guide through this work

I have decided to pick up three to my mind important realizations of the so called Berry phase. The first is the original derivation of Berry [8], which points out that a system which evolves cyclically under an adiabatic condition picks up an additional phase factor which turns out to be geometrical in nature. Due to the special adiabatic condition Aharonov and Anandan [2] try to remove this condition and to generalize the occurrence of the the phase to evolutions that have to fulfill only the cyclic condition. This is treated in the second part of my work. The third part is dedicated to Pancharatnam [56], who found several years before Berry's derivation a geometrical phase in connection with different states of polarized light. This can be seen as a generalization of Berry's phase for nonclosed loops, so to say for noncyclic evolution. Each part contains a general derivation of the ideas and then an application to a special physical example, the spin-$\frac{1}{2}$ particle in a rotating magnetic field and quantum measurements.

The next part of my work considers some experimental setups. There is a wide range of experiments concerning geometrical phases, therefore I have picked up two experiments with photons and two with neutrons, which I discuss in detail. A list of further experiments completes this part.

In the following I give an inside on some applications of the Berry phase. First I discuss an application on entangled spin $\frac{1}{2}$ systems, which is rather uncommented in literature. There I give an example of a Bell inequality where I applied Berry's phase, too. Then I concentrate on a really important part for future investigations: the quantum computer. There the Berry phase offers a possibility to construct fault tolerant quantum gates.

The last chapter is dedicated to geometry. After a brief introduction into the concept of differential geometry and the fibre bundles formalism I treat the formulation of the Berry phase in this geometrical language. This is a very elegant formulation which allows a rather natural understanding of geometrical phases and their properties.

Chapter 2

The Berry phase

2.1 Introduction

In 1984 Berry published a paper [8] which has until now deeply influenced the physical community. Therein he considers cyclic evolutions of systems under special conditions, namely adiabatic ones. He finds that an additional phase factor occurs in contrast to the well known dynamical phase factor. This phenomenon can be described by "global change without local change". Berry points out the geometrical character of this phase which is not be negligible because of its nonintegrable character. But this was not the first time that someone found such a phase factor[1]. Considerations, for instance, of the Born-Oppenheimer approximation done by Mead and Truhlar in 1979 [46] revealed also this additional phase factor but it had been neglected. Berry showed that this was not correct because the phase is gauge invariant and therefore can not be gauged away. Since this much work has been done to this issue and the so called Berry phase is now well established, theoretically as well as experimentally (see chapter 5).

2.2 Derivation

We consider a quantum system described by a Hamiltonian H that depends on a multidimensional real parameter R which parametrizes the environment of the system. The time evolution is described by the timedependent Schrödinger equation

$$H(R(t))|\psi(t)\rangle = i\hbar\frac{\partial}{\partial t}|\psi(t)\rangle \tag{2.2.1}$$

We can choose at any instant a basis of eigenstates $|n(R(t))\rangle$ for the Hamiltonian labelled by the quantum number n such that the eigenvalue equation is fulfilled

$$H(R(t))|n(R(t))\rangle = E_n(R(t))|n(R(t))\rangle \tag{2.2.2}$$

[1]For a detailed discussion of the anticipations of Berry's phase see [10].

We assume that the energy spectrum of H is discrete, that the eigenvalues are not degenerated and that no level crossing occurs during the evolution. Suppose the environment and therefore $R(t)$ is adiabatically varied, that means the changes happen slowly in time compared to the characteristic time scale of the system. The system starts in the n-th energy eigenstate

$$|\psi(0)\rangle = |n(R(0))\rangle \tag{2.2.3}$$

then according to the adiabatic theorem the system stays over the whole evolution in the n-th eigenstate of the instant Hamiltonian. But it is possible that the state gains some phase factor which does not affect the physical state. Therefore the state of the system can be written as

$$|\psi(t)\rangle = e^{i\phi_n}|n(R(t))\rangle \tag{2.2.4}$$

One would expect that this phase factor is identical with the dynamical phase factor θ_n which is the integral over the energy eigenvalues

$$\theta_n(t) = -\frac{1}{\hbar}\int_0^t E_n(t')dt' \tag{2.2.5}$$

but it is not forbidden by the adiabatic theorem and the Schrödinger equation to add another term γ_n which is called the Berry phase

$$\phi_n(t) = \theta_n(t) + \gamma_n(t) \tag{2.2.6}$$

We can determine this additional term by inserting the ansatz (2.2.4) together with equation (2.2.6) into the Schrödinger equation (2.2.1). This yields with the simplifying notation $R \equiv R(t)$

$$\frac{\partial}{\partial t}|n(R)\rangle + i\frac{d}{dt}\gamma_n(t)|n(R)\rangle = 0 \tag{2.2.7}$$

After taking the inner product (which should be normalized) with $\langle n(R)|$ we get

$$\begin{aligned} \frac{d}{dt}\gamma_n(t) &= i\langle n(R)|\frac{\partial}{\partial t}|n(R)\rangle \\ \frac{d}{dt}\gamma_n(t) &= i\langle n(R)|\nabla_R|n(R)\rangle\frac{dR}{dt} \end{aligned} \tag{2.2.8}$$

and after the integration

$$\gamma_n(t) = i\int_{R_i}^{R_f}\langle n(R)|\nabla_R|n(R)\rangle dR \tag{2.2.9}$$

If we now consider cyclic evolutions around a closed circuit C in a time T such that $R(0) = R(T)$ then the Berry phase looks like the following

$$\gamma_n(C) = i\oint_C \langle n(R)|\nabla_R|n(R)\rangle dR \tag{2.2.10}$$

This quantity can not be written as a function of R therefore it is nonintegrable. It is not single valued, this means although we come back to the starting point in parameterspace by going a closed circuit the Berry phase is unequal to zero.

Another important point is that the Berry phase depends on the circuit C traced out in parameterspace but not on the way the circuit is traversed and it is independent of the velocity of the traverse. We can see it as a geometrical property of the system or the underlying parameterspace and can describe it within differential geometry as a holonomy of the parallel transported eigenstates (see section 7.3).

The normalization of $|n(R)\rangle$ ensures that $\gamma_n(C)$ is real. This can be easily shown by

$$\begin{aligned} \nabla_R\langle n|n\rangle &= 0 \\ \langle\nabla_R\, n|n\rangle + \langle n|\nabla_R\, n\rangle &= \langle n|\nabla_R\, n\rangle^* + \langle n|\nabla_R\, n\rangle = 0 \\ 2\cdot\Re e\langle n|\nabla_R\, n\rangle &= 0 \end{aligned} \tag{2.2.11}$$

From this we see that $\langle n|\nabla_R\, n\rangle$ is purely imaginary because the real part is equal to zero. Therefore γ_n has to be real.

Furthermore if the parameterspace is simply connected and it is possible to choose $|n(R)\rangle$ everywhere real in a smooth way, then $\gamma_n(C)$ is zero.

2.3 Berry phase as a gauge potential

It is appropriate for further discussions and for the geometrical considerations in section 7.3 to reformulate the Berry phase, equation (2.2.10), as a $U(1)$ gauge potential. This can be done in the following way

$$\gamma_n(C) = \oint_C A_n dR \tag{2.3.1}$$

where the gauge potential A_n is given by

$$A_n(R) = i\langle n(R)|\nabla_R|n(R)\rangle \tag{2.3.2}$$

It is now easy to see that the Berry phase is a gauge invariant object under the following gauge transformation of the eigenstates

$$|n(R)\rangle \to |n(R)\rangle' = e^{i\xi_n(R)}|n(R)\rangle \tag{2.3.3}$$

where $\xi_n(R)$ is an arbitrary but single valued real phase. The new objects $|n(R)\rangle'$ also form a basis of eigenstates of the Hamiltonian. If we insert the transformation into equation (2.3.2) we get the following modification for the gauge potential

$$A_n(R) \to A'_n(R) = A_n(R) - \nabla_R\xi_n(R) \tag{2.3.4}$$

This gives no change for the Berry phase

$$\gamma_n(R) \to \gamma'_n(R) = \gamma_n(R) \tag{2.3.5}$$

when we assume that $\xi_n(R)$ is a single valued function. We see that the Berry phase is invariant with respect to the gauge transformation (2.3.3) of the basis vectors. The Berry phase is a gauge invariant object and it is not possible to remove it by a certain choice of the basis states of the Hamiltonian.

We can conclude from this: We introduce a phase factor in addition to the dynamical phase factor that does not contradict the adiabatic theorem nor the eigenvalue equation. It turns out that this phase factor is essential and can not be ignored because of its invariance under U(1)-transformations.

2.4 Comment on the adiabatic theorem

The adiabatic theorem is first mentioned by Ehrenfest [31], who studies adiabatic processes in mechanics and the early quantum mechanics. Therefore it is also sometimes called Ehrenfest theorem[2]. The first proof is given by Born and Fock [21] in 1928. In 1950 Kato [42] considers adiabatic evolutions in quantum systems and gives a proof of the adiabatic theorem in quantum mechanics. In 1959 also Messiah in his famous book about quantum mechanics [47] treats the adiabatic approximation. In the quantum mechanic book of Griffiths [36] we find a plausible argument for the adiabatic approximation and Aguiar-Pinto et al. [1] calculate the phase for the spin-$\frac{1}{2}$ model and show explicitly that the adiabatic limit of the solution gives the desired result of the adiabatic approximation.

An exact proof of the adiabatic theorem is not easy. If we go back to section 2.2 we see that in equation (2.2.4) we have used the adiabatic assumption. In general the time evolved state is a sum over all possible eigenstates

$$|\psi(t)\rangle = \sum_{n=1}^{N} e^{i\gamma_n} e^{i\theta_n} |n(R(t))\rangle \tag{2.4.1}$$

By inserting this into the time dependent Schrödinger equation (2.2.1) we get the following coupled differential equations for the phase $\gamma_n(t)$

$$\begin{aligned} \frac{d}{dt}\gamma_n(t) e^{i\gamma_n} e^{i\theta_n} &= \sum_{m=1}^{N} i e^{i\gamma_m} e^{i\theta_m} \langle n(R)| \frac{\partial}{\partial t} |m(R)\rangle \\ &= i e^{i\gamma_n} e^{i\theta_n} \langle n(R)| \frac{\partial}{\partial t} |n(R)\rangle + \sum_{m\neq n} i e^{i\gamma_m} e^{i\theta_m} \langle n(R)| \frac{\partial}{\partial t} |m(R)\rangle \end{aligned} \tag{2.4.2}$$

We see that if the transitions into other eigenstates can be neglected then the second part of the sum can be neglected and we get back to the well known equation of the Berry phase equation (2.2.8). This approximation is also valid in the adiabatic regime which can be characterized by slow evolution of the system compared to the intrinsic time scale of the system. Mathematically spoken this can be expressed by $\frac{\omega_0}{\omega_i} \to 0$ where ω_0 denotes the angular frequency of the evolution and ω_i is the intrinsic frequency of the system, for instance the difference between two distinct energy values divided by $\hbar$.

[2] See [47] p.224, footnote 4.

2.5 Wilczek-Zee gauge potential

In section 2.2 we only considered nondegenerate Hamiltonians. In 1984 Wilczek and Zee [80] generalized Berry's formula for degenerate Hamiltonians. This leads to non-abelian gauge field.

The Hilbertspace is a direct sum of all eigenspaces V_n associated with the corresponding eigenvalue E_n

$$\mathcal{H} = \oplus_n V_n \tag{2.5.1}$$

In the nondegenerate case these eigenspaces are all one-dimensional. If there occurs a k-fold degeneracy, for example in the n-th eigenvalue, then the corresponding eigenspace V_n is k-dimensional. The eigenspace depends via the eigenvalue equation on the external parameter R and evolves in time. An evolution is called cyclic with a period T, when for $R(0) = R(T)$ also the eigenspaces coincide $V_n(0) = V_n(T)$. We can find an orthonormal basis $\{|\psi_a(t)\rangle, a = 1, \ldots, n\}$ for $V_n(t)$ by

$$H(R(t))|\psi_a(t)\rangle = E_n(R(t))|\psi_a(t)\rangle \tag{2.5.2}$$

We demand that this basis is single valued for every a

$$|\psi_a(T)\rangle = |\psi_a(0)\rangle \tag{2.5.3}$$

Every state vector $|\Psi_n(t)\rangle$ which is lying in the n-th eigenspace is described by the timedependent Schrödinger equation

$$i\hbar\frac{\partial}{\partial t}|\Psi_n(t)\rangle = H(t)|\Psi_n(t)\rangle \tag{2.5.4}$$

with the initial condition

$$|\Psi_n(0)\rangle = |\psi_a(0)\rangle \tag{2.5.5}$$

where $|\psi_a(0)\rangle \in V_n(0)$. We can decompose the time evolved state vector into a linearcombination of the single valued basisvectors

$$|\Psi_n(t)\rangle = \sum_a U_{na}(t)|\psi_a(t)\rangle \tag{2.5.6}$$

where U_{na} denotes a unitary mixing matrix[3], which we want to determine later on. In this decomposition we have already used the adiabatic limit, because we stayed in one energy eigenspace and considered no transitions into other eigenspaces.

If we insert equation (2.5.6) into the timedependent Schrödinger equation (2.5.4) and multiply it with $\langle\Psi_n(t)|$ (which we assume to be normalized) we get with the

[3]The mixing occurs between different basis states $|\psi_a\rangle$ of an eigenspace but not between different eigenspaces.

help of equation (2.5.2) the following results[4]

$$\begin{aligned}
\langle\Psi_n|\frac{\partial}{\partial t}|\Psi_n\rangle &= \frac{E_n}{i\hbar} \\
\langle\Psi_n|\frac{\partial}{\partial t}U_{nb}|\psi_b\rangle + \langle\Psi_n|U_{nb}\frac{\partial}{\partial t}|\psi_b\rangle &= \frac{E_n}{i\hbar} \\
\langle\psi_a|U_{an}^{-1}\frac{\partial}{\partial t}U_{nb}|\psi_b\rangle + \langle\psi_a|U_{an}^{-1}U_{nb}\frac{\partial}{\partial t}|\psi_b\rangle &= \frac{E_n}{i\hbar} \\
\langle\psi_a|U_{an}^{-1}\frac{\partial}{\partial t}U_{nb}|\psi_b\rangle + \langle\psi_a|\delta_{n;ab}\frac{\partial}{\partial t}|\psi_b\rangle &= \frac{E_n}{i\hbar}
\end{aligned} \tag{2.5.7}$$

where we have used $U_{an}^{-1}U_{nb} = \delta_{n;ab}$ which denotes the ab-component of the k-dimensional unit-matrix of the n-th eigenspace. We can further introduce the anti-hermitian matrix A which plays the role of a gauge potential. It is defined by

$$A_{n;ab} = (U^{-1}\frac{\partial}{\partial t}U)_{n;ab} = (\frac{E_n}{i\hbar} - \frac{\partial}{\partial t})\delta_{n;ab} \tag{2.5.8}$$

This gives a differential equation for U_n which is solved by the path-ordered integral

$$U_n(t) = \mathcal{P}e^{\int_0^t A_n(t')dt'} \tag{2.5.9}$$

where $\mathcal{P}$ denotes path-ordering and $A_n = \langle\psi_a|A_{n;ab}|\psi_b\rangle$. The gauge potential A_n can be decomposed into the dynamical part and the geometrical part, which can be interpreted as the non-abelian generalization of the Berry phase

$$\begin{aligned}
A_n &= \frac{k}{i\hbar}E_n - \langle\psi_a|\frac{\partial}{\partial t}|\psi_a\rangle \\
&= \theta_n + \gamma_n
\end{aligned} \tag{2.5.10}$$

The phase factor U_n (which includes also a dynamical part) represents the generalization of the Berry phase to the general group U(k). It is also a pure geometrical object and depends therefore only on the geometry of the degenerate space. Under a unitary transformation of the basis vectors

$$|\psi_b'(t)\rangle = \Omega(t)_{n;ba}|\psi_a(t)\rangle \tag{2.5.11}$$

where $\Omega_{n;ba}(t)$ is a unitary matrix, the gauge potential transforms in the following way

$$A_n'(t) = \Omega_n^{-1}A_n\Omega_n + \Omega_n^{-1}\dot{\Omega}_n \tag{2.5.12}$$

This is just the transformation law for a nonabelian gauge transformation. We can rewrite equation (2.5.9) in terms of the parameter R and with the in the parameterspace closed loop C in the following way

$$U(t) = \mathcal{P}e^{\oint_C A(R)dR} \tag{2.5.13}$$

This integral is also called a Wilsonloop.

[4]We have used Einstein's summation convention: over indices that occur twice is summed.

2.6 Example: spin-$\frac{1}{2}$ particle in an adiabatically rotating magnetic field

We apply the Berry phase to a concrete and very important example. We consider a spin-$\frac{1}{2}$ particle moving in an external magnetic field $\vec{B}$ which rotates adiabatically (slowly) under an angle ϑ around the z-axis. The magnetic field is given by

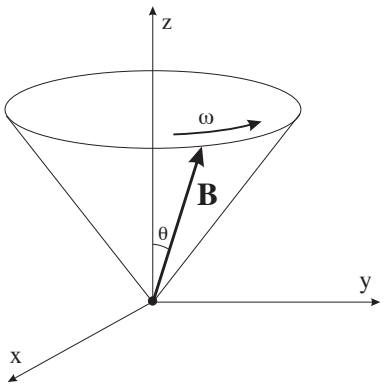

Figure 2.1: Spin-$\frac{1}{2}$ particle in the magnetic field described by equation (2.6.1).

$$\vec{B}(t) = B_0 \begin{pmatrix} \sin\vartheta\cos(\omega t) \\ \sin\vartheta\sin(\omega t) \\ \cos\vartheta \end{pmatrix} \tag{2.6.1}$$

where ω is the angular frequency of the rotation and $B_0 = |\vec{B}(t)|$. When the field rotates slowly enough, then the spin of the particle will follow the direction of the field, an eigenstate of $H(0)$ stays for later times t an eigenstate of $H(t)$. The interaction Hamiltonian for this system in the rest frame is given by

$$\begin{aligned} H(t) &= \mu\vec{B}\cdot\vec{\sigma} \\ H(t) &= \mu B_0 \begin{pmatrix} \cos\vartheta & e^{-i\omega t}\sin\vartheta \\ e^{i\omega t}\sin\vartheta & -\cos\vartheta \end{pmatrix} \end{aligned} \tag{2.6.2}$$

with the constant $\mu = \frac{1}{2}\frac{e}{m}\hbar$. The eigenvalue equation

$$H(t)|n(t)\rangle = E_n|n(t)\rangle \tag{2.6.3}$$

is solved by the following normalized eigenstates of $H(t)$

$$\begin{aligned} |n_+(t)\rangle &= \begin{pmatrix} \cos\frac{\vartheta}{2} \\ e^{i\omega t}\sin\frac{\vartheta}{2} \end{pmatrix} \\ |n_-(t)\rangle &= \begin{pmatrix} -\sin\frac{\vartheta}{2} \\ e^{i\omega t}\cos\frac{\vartheta}{2} \end{pmatrix} \end{aligned} \tag{2.6.4}$$

with the corresponding energy eigenvalues

$$E_\pm = \pm\mu B_0 \tag{2.6.5}$$

We can interpret the eigenstates as spin-up $|n_+(t)\rangle \equiv |\Uparrow_{\vec{B}(t)}\rangle$ and spin-down $|n_-(t)\rangle \equiv |\Downarrow_{\vec{B}(t)}\rangle$ along the respective $\vec{B}(t)$-direction.

The Hamiltonian depends on $\vec{B}(t)$ which is described by ϑ, $\phi(t) = \omega t$ and $r = B_0$. This means the parameterspace is identical with the allowed values of $\vec{B}(t)$ which forms a S^2. In our special configuration $\vec{B}(t)$ traces out the curve C which is visualized in figure 2.2.

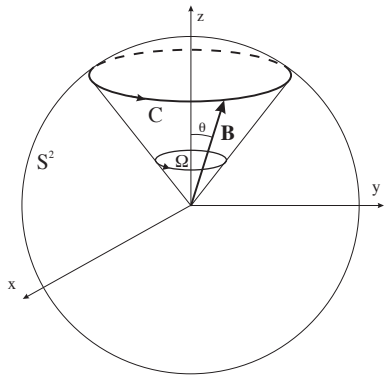

Figure 2.2: Parameterspace for the magnetic field described by equation (2.6.1).

The gradient in the parameterspace spanned by $\vec{B}(t)$ is given by the following expression

$$\nabla|n_\pm(t)\rangle = \frac{\partial}{\partial r}|n_\pm(t)\rangle\hat{r} + \frac{1}{r}\frac{\partial}{\partial\vartheta}|n_\pm(t)\rangle\hat{\vartheta} + \frac{1}{r\sin\vartheta}\frac{\partial}{\partial\phi}|n_\pm(t)\rangle\hat{\phi} \tag{2.6.6}$$

This gives for the eigenstates (2.6.4)

$$\begin{aligned}\nabla|n_+(t)\rangle &= \frac{1}{r}\begin{pmatrix}-\frac{1}{2}\sin\frac{\vartheta}{2}\\ \frac{1}{2}e^{i\omega t}\cos\frac{\vartheta}{2}\end{pmatrix}\hat{\vartheta} + \frac{1}{r\sin\vartheta}\begin{pmatrix}0\\ ie^{i\omega t}\sin\frac{\vartheta}{2}\end{pmatrix}\hat{\phi}\\ \nabla|n_-(t)\rangle &= \frac{1}{r}\begin{pmatrix}-\frac{1}{2}\cos\frac{\vartheta}{2}\\ -\frac{1}{2}e^{i\omega t}\sin\frac{\vartheta}{2}\end{pmatrix}\hat{\vartheta} + \frac{1}{r\sin\vartheta}\begin{pmatrix}0\\ ie^{i\omega t}\cos\frac{\vartheta}{2}\end{pmatrix}\hat{\phi}\end{aligned} \tag{2.6.7}$$

The scalar product with the corresponding $\langle n|$ gives

$$\begin{aligned}\langle n_+|\nabla|n_+\rangle &= i\,\frac{\sin^2(\frac{\vartheta}{2})}{r\sin\vartheta}\,\hat{\phi}\\ \langle n_-|\nabla|n_-\rangle &= i\,\frac{\cos^2(\frac{\vartheta}{2})}{r\sin\vartheta}\,\hat{\phi}\end{aligned} \tag{2.6.8}$$

The integration along the curve C

$$C : r = constant, \vartheta = constant, \phi \in [0, 2\pi] \tag{2.6.9}$$

gives

$$\oint_C \langle n_\pm|\nabla|n_\pm\rangle\, r\sin\vartheta\; d\phi\;\hat{\phi} = i\,\pi(1 \mp \cos\vartheta) \tag{2.6.10}$$

The Berry phase equation (2.2.10) has then the following form

$$\gamma_{\pm}(C) = -\pi(1 \mp \cos\vartheta) \tag{2.6.11}$$

This can be expressed in terms of the solid angle $\Omega = \int_0^{2\pi}(1 - \cos\vartheta(\phi))\ d\phi$ in the following way

$$\gamma_{\pm}(C) = \mp\frac{1}{2}\Omega(C) \qquad \mod 2\pi \tag{2.6.12}$$

The dynamical phase for one rotation within a period $T = \frac{2\pi}{\omega}$ is given by

$$\theta_{\pm}(T) = -\frac{1}{\hbar}\int_0^T E_{\pm}(t)dt = \mp\frac{\mu}{\hbar}B_0 T \tag{2.6.13}$$

The total state after one rotation where $\vec{B}(T) = \vec{B}(0)$ is then given by

$$|n_{\pm}(T)\rangle = e^{-i\pi(1\mp\cos\vartheta)}e^{\mp i\frac{\mu}{\hbar}B_0 T}|n_{\pm}(0)\rangle \tag{2.6.14}$$

We see that the dynamical phase depends on the period T of the rotation but the geometrical phase depends only on the special geometry of the problem – in this case the opening angle ϑ of the cone that the magnetic field traces out (see figure 2.2).

Chapter 3

The Aharonov-Anandan phase

3.1 Generalization of Berry's phase

In 1987 Aharonov and Anandan [2] proposed an important generalization of Berry's phase. They consider cyclic evolutions that are not restricted by an adiabatic condition. This means that we need no parameterspace to describe the cyclic evolution of the Hamiltonian but only the projective Hilbert space where the system traces out closed curves. Berry's phase is then a special case of this so called Aharonov-Anandan phase. This generalization is very important, because in real processes the adiabatic condition is never exactly fulfilled. This is also the reason why Berry tried to remove the adiabatic condition by calculating adiabatic correction terms [9]. Soon after the work of Aharonov and Anandan several other generalizations occurred which are not treated in this work. For example, Samuel and Bhandari [61] removed the cyclic condition[1] and Garrison and Chiao [35] showed that geometrical phases also occur in any classical complex multicomponent field, that satisfies nonlinear equations derived from a Lagrangian which is invariant under gauge transformations of the first kind. That means also in classical theories the pendants of quantal phases exist and are known as Hannay angles [37].

3.2 Phase conventions

In quantum physics the physical state of a system is only determined up to a phase. Physical states are defined as equivalence classes of the vectors in Hilbert space, which are called the projective Hilbert space. When a system evolves in time it is described by the time dependent Schrödinger equation. The solution of this differential equation is given by a phase factor times the initial state. This phase factor is called the dynamical one, because it comes from the dynamics of the system. But as we have see in chapter 2 also other additional phase factors can occur. The total phase a system gains during its evolution, which is the only measurable quantity, is a sum of the dynamical and the geometrical phase. The most common way to define

[1] This work stands in deep connection to Pancharatnam's work (see chapter 4).

the geometrical phase is to set it as the difference of the total and the dynamical phase, where the dynamical phase is due to definition (compare (2.2.5)) given by

$$\theta(T) = -\frac{1}{\hbar}\int_0^T \langle\psi(t)|H(t)|\psi(t)\rangle dt \tag{3.2.1}$$

But it is also possible to do it the other way round, to define first the geometrical phase and then identify the dynamical phase as the complement to the total phase. This division is in a way historically grown because as we will see in the general evolution of a system the geometrical part has also a dependence on parameters of the Hamiltonian and not only on parameters that describe the path traced out (see section 3.4). Of physical relevance in an experiment is only the total phase. The respective part of the phase can only be measured if the other part is set to zero due to the corresponding experimental setup or if it stays constant during the whole experiment, as it is done in an interferometer where the dynamical phase is for both arms the same.

3.3 Derivation

We[2] consider the projective Hilbert space $\mathcal{P}$, which is built up of the equivalence classes of all state vectors of the Hilbert space $\mathcal{H}$. We can define the projection map Π from the Hilbertspace into the projective Hilbertspace by

$$\begin{aligned} &\Pi : \mathcal{H} \to \mathcal{P} \\ &\Pi(|\psi\rangle) = \{|\psi'\rangle : |\psi'\rangle = c|\psi\rangle, c \in \mathbb{C}\} \end{aligned} \tag{3.3.1}$$

This means all "rays" of $\mathcal{H}$ that represent all possible state vectors are mapped onto one representative in $\mathcal{P}$ (see figure 3.1(a)).

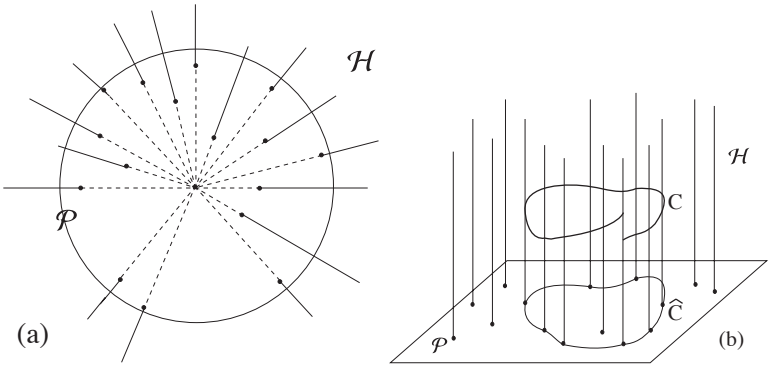

Figure 3.1: (a) An illustration of the projective Hilbertspace. (b) A cyclic evolution in the projective Hilbertspace and in the Hilbert space.

The density-matrix operator ρ

$$\rho(t) = |\psi(t)\rangle\langle\psi(t)| \tag{3.3.2}$$

[2]This section follows reference [44].

corresponds to to the projective Hilbertspace because any phase information is lost.

We consider a cyclic evolution of a state vector $|\psi(t)\rangle$ with a period T in the projective space. That means the evolution traces out an arbitrary curve C in the Hilbertspace $\mathcal{H}$ but the projection of this curve gives a closed curve $\hat{C} = \Pi(C)$ in $\mathcal{P}$ (see figure 3.1(b)). Then the final state differs from the initial state only by a phase factor

$$|\psi(T)\rangle = e^{i\Phi}|\psi(0)\rangle \tag{3.3.3}$$

The state vector $|\psi(t)\rangle$ evolves according to the Schrödinger equation which gives in general an open curve in $\mathcal{H}$. In the projective space $\mathcal{P}$ we have the vector $|\xi(t)\rangle$ which forms the curve $\hat{C} = \Pi(C)$ and therefore is single valued

$$|\xi(T)\rangle = |\xi(0)\rangle \tag{3.3.4}$$

The vectors in $\mathcal{H}$ are obtained by a multiplication with an appropriate complex factor $f(t)$

$$|\psi(t)\rangle = e^{if(t)}|\xi(t)\rangle \tag{3.3.5}$$

which has to fulfill the following relation

$$f(T) - f(0) = \Phi \tag{3.3.6}$$

When we insert equation (3.3.5) into the Schrödinger equation (2.2.1) we obtain the equations of motions for $f(t)$ and $|\xi(t)\rangle$

$$i\hbar\frac{d}{dt}|\xi(t)\rangle = (H + \hbar\dot{f})|\xi(t)\rangle \tag{3.3.7}$$

$$\hbar\frac{d}{dt}f(t) = i\langle\xi|\frac{\partial}{\partial t}|\xi\rangle - \langle\xi|H|\xi\rangle \tag{3.3.8}$$

After integrating equation (3.3.8) from 0 to T we get

$$\int_0^T \frac{d}{dt}f(t)dt = \Phi = \theta + \beta \tag{3.3.9}$$

where we have already used that the total phase consists of two parts. In this case there arises a natural identification due to equation (3.3.8) into a dynamical and a geometrical part. The dynamical phase is given by

$$\theta = -\frac{1}{\hbar}\int_0^T \langle\xi|H|\xi\rangle dt = -\frac{1}{\hbar}\int_0^T \langle\psi|H|\psi\rangle dt \tag{3.3.10}$$

and the geometrical phase, the so called Aharonov-Anandan phase, writes as

$$\beta = i\oint_{\hat{C}} \langle\xi|\frac{\partial}{\partial t}|\xi\rangle dt \tag{3.3.11}$$

In this derivation we have not used the adiabatic condition. The phase also arises when the Hamiltonian is not cyclic, $H(T) \neq H(0)$. It only depends on the cyclicity of the time evolution of the system. Another advantage is that the initial state needs not to be an eigenstate of the Hamiltonian, hence the Aharonov-Anandan phase is

valid for arbitrary state vectors. In the adiabatic limit the Aharonov-Anandan phase goes over into the Berry phase.

The Aharonov-Anandan phase does not depend on the concrete form of the Hamiltonian. The parametrisation of the curve $\hat{C}$ has no effect on the value of the phase and it is uniquely defined up to a factor 2π. The phase only depends on the curve $\hat{C}$ and the geometry of the projective Hilbertspace $\mathcal{P}$ in contrast to the Berry phase which depends on the geometry of the parameterspace.

3.4 Example: spin-$\frac{1}{2}$ particle in an arbitrary rotating magnetic field

Lets come back to the example of a spin $\frac{1}{2}$-particle in a rotating magnetic field. To apply the Aharonov-Anandan construction[3] we do not need to assume any adiabatic restriction to the angular frequency ω. This means the magnetic field looks like the following where all possible angular frequencies ω are allowed

$$\vec{B}(t) = B_0 \begin{pmatrix} \sin\vartheta\cos(\omega t) \\ \sin\vartheta\sin(\omega t) \\ \cos\vartheta \end{pmatrix} = B_0\vec{e}(\vartheta, \omega t) \tag{3.4.1}$$

The Hamiltonian for this system is again

$$H(t) = \mu\vec{B}\cdot\vec{\sigma} = \mu B_0 \begin{pmatrix} \cos\vartheta & e^{-i\omega t}\sin\vartheta \\ e^{i\omega t}\sin\vartheta & -\cos\vartheta \end{pmatrix} \tag{3.4.2}$$

We consider the general evolution of an arbitrary state $|\psi\rangle$ described by the timedependent Schrödinger equation

$$H(t)|\psi(t)\rangle = i\hbar\frac{\partial}{\partial t}|\psi(t)\rangle \tag{3.4.3}$$

To solve this equation we transform into the bodyfixed system, which rotates with the field at an angular frequency ω and make the following ansatz

$$|\psi(t)\rangle = e^{-i\frac{\sigma_z}{2}\omega t}|\eta(t)\rangle \tag{3.4.4}$$

with the initial condition $|\psi(0)\rangle = |\eta(0)\rangle$. For this new state $|\eta(t)\rangle$ a modified Schrödinger equation holds

$$\bar{H}|\eta(t)\rangle = i\hbar\frac{\partial}{\partial t}|\eta(t)\rangle \tag{3.4.5}$$

with the time independent Hamiltonian

$$\bar{H} = \bar{H}(\omega) = H(t=0) - \frac{\hbar\omega}{2}\sigma_z = \begin{pmatrix} \mu B_0\cos\vartheta - \frac{\hbar\omega}{2} & \mu B_0\sin\vartheta \\ \mu B_0\sin\vartheta & -\mu B_0\cos\vartheta - \frac{\hbar\omega}{2} \end{pmatrix} \tag{3.4.6}$$

[3]This section follows reference [19, 74].

The coupling can be written in the same form as equation (3.4.2) by using a new magnetic field $\vec{B}'$

$$\bar{H} = \mu \vec{B}' \vec{\sigma} \tag{3.4.7}$$

which is given by

$$\vec{B}' = \bar{B}_0 \begin{pmatrix} \sin\bar{\vartheta} \\ 0 \\ \cos\bar{\vartheta} \end{pmatrix} = \bar{B}_0 \vec{e}(\bar{\vartheta}, 0) \tag{3.4.8}$$

It is not so difficult to get the right transformations for the new variables

$$\bar{B}_0 = B_0 \Delta \tag{3.4.9}$$

$$\sin\bar{\vartheta} = \frac{\sin\vartheta}{\Delta} \tag{3.4.10}$$

$$\cos\bar{\vartheta} = \frac{\cos\vartheta}{\Delta} - \frac{\hbar\omega}{2B_0\mu\Delta} \tag{3.4.11}$$

where the scaling factor Δ is given by

$$\Delta = \sqrt{1 - \frac{\hbar\omega}{\mu B_0}\cos\vartheta + \frac{\hbar^2\omega^2}{4\mu^2 B_0^2}} = \frac{\bar{B}_0}{B_0} \tag{3.4.12}$$

Equation (3.4.5) can be solved simply by integration because the Hamilton is time independent and we get

$$|\eta(t)\rangle = e^{-\frac{i}{\hbar}\bar{H}t}|\eta(0)\rangle \tag{3.4.13}$$

This result we insert into equation (3.4.4) which gives us the solution for the state $|\psi(t)\rangle$

$$|\psi(t)\rangle = e^{-i\frac{\sigma_z}{2}\omega t} e^{-\frac{i}{\hbar}\bar{H}t}|\psi(0)\rangle \tag{3.4.14}$$

We consider now a cyclic evolution with a period $T = \frac{2\pi}{\omega}$. We can compute the dynamical and the geometrical phase with the state vector (3.4.14) and (3.4.13). To simplify the calculation we choose the initial state to be an eigenstate of the time independent Hamiltonian $\bar{H}$. We can write down the following eigenvalue equations

$$\bar{H}|\eta_\pm\rangle = E_\pm|\eta_\pm\rangle \tag{3.4.15}$$

$$\sigma_z|\pm\rangle = \pm|\pm\rangle \tag{3.4.16}$$

where the two eigenstates are related by

$$|\eta_\pm\rangle = e^{-i\bar{\vartheta}\frac{\sigma_y}{2}}|\pm\rangle \tag{3.4.17}$$

The initial state is then given by

$$|\psi(0)\rangle = |\eta_\pm\rangle \tag{3.4.18}$$

According to equation (3.4.14) we get

$$\begin{aligned} |\psi(T)\rangle =& e^{-i\frac{\sigma_z}{2}\omega T} e^{-\frac{i}{\hbar}\bar{H}T}|\eta_\pm\rangle \\ =& e^{-i\sigma_z\pi} e^{-\frac{i}{\hbar}E_\pm T}|\eta_\pm\rangle \\ =& e^{\mp i\pi} e^{-\frac{i}{\hbar}E_\pm T}|\eta_\pm\rangle \end{aligned} \tag{3.4.19}$$

We can interpret this as a total phase factor

$$|\psi(T)\rangle = e^{i\phi(T)}|\eta_\pm\rangle \tag{3.4.20}$$

where the total phase is given by

$$\phi(T) = -\frac{1}{\hbar}E_\pm T \mp \pi \tag{3.4.21}$$

This phase can be split up (according to section 3.3) into a dynamical and a geometrical part. We define the dynamical part to be the expectation value of the Hamiltonian $H(t)$

$$\begin{aligned}\theta(T) &= -\frac{1}{\hbar}\int_0^T \langle\psi(t)|H(t)|\psi(t)\rangle dt = -\frac{1}{\hbar}\int_0^T \langle\eta_\pm|H(t)|\eta_\pm\rangle dt \\ &= -\frac{1}{\hbar}\int_0^T \left(\langle\eta_\pm|\bar{H}|\eta_\pm\rangle dt + \frac{\hbar\omega}{2}\langle\eta_\pm|\sigma_z|\eta_\pm\rangle\right) dt\end{aligned} \tag{3.4.22}$$

Then we compute the geometrical part as the difference between total phase and dynamical phase. We have used the transformation into the bodyfixed system

$$H = \bar{H} + \frac{\hbar\omega}{2}\sigma_z \tag{3.4.23}$$

The first part of the integral gives the energy eigenvalue. The second part is related to the spin expectation value along the rotation axis, the so called spin alignment. We can compute it with the help of the following relation

$$e^{i\vartheta\frac{\sigma_y}{2}}\sigma_z e^{-i\vartheta\frac{\sigma_y}{2}} = \sigma_z\cos\vartheta - \sigma_x\sin\vartheta \tag{3.4.24}$$

therefore we get for the spin alignment

$$\begin{aligned}\langle\eta_\pm|\sigma_z|\eta_\pm\rangle &= \langle\pm|e^{i\bar{\theta}\frac{\sigma_y}{2}}\sigma_z e^{-i\bar{\theta}\frac{\sigma_y}{2}}|\pm\rangle \\ &= \langle\pm|\big(\cos\bar{\vartheta}\sigma_z - \sin\bar{\vartheta}\sigma_x\big)|\pm\rangle \\ &= \pm\cos\bar{\vartheta}\end{aligned} \tag{3.4.25}$$

Therefore we get for the dynamical phase

$$\begin{aligned}\theta(T) &= -\frac{1}{\hbar}\int_0^T \big(E_\pm \pm \frac{\hbar\omega}{2}\cos\bar{\vartheta}\big)dt \\ &= -\frac{1}{\hbar}E_\pm T \mp \pi\cos\bar{\vartheta}\end{aligned} \tag{3.4.26}$$

The geometrical phase, in this case the Aharonov-Anandan phase, is given by

$$\begin{aligned}\beta(T) &= \phi(T) - \theta(T) \\ &= \mp\pi(1-\cos\bar{\vartheta})\end{aligned} \tag{3.4.27}$$

This formula looks quite similar to the one of the Berry phase. The only difference is that in this case it is defined with another angel $\bar{\vartheta}$. In the adiabatic limit, where $\omega \ll \mu B_0$, the two angles are identical and hence the two phases.

Chapter 4

The Pancharatnam phase

4.1 Introduction

In 1956 Pancharatnam[1] published a paper [56] about the interference of polarized light. Therein he defines the phase difference of two nonorthogonal states of polarization. Two states are in phase if the intensity of the superposed state reaches a maximum. In other words, the phase difference between two beams is defined as the phase change which has to be applied to one beam in order to maximize the intensity of their superposition. It turns out that this phase has also geometrical properties. One can think of this as the earliest appearance of a geometrical phase definition in literature. This was pointed out by Ramaseshan and Nityananda [58] in 1986. With this concept one is able to define geometrical phases also for evolutions that are not limited to the cyclic condition, as Samuel and Bhandari [61] showed. The Pancharatnam phase has already been confirmed in many experiments (see section 5.3).

4.2 Poincaré sphere

Pancharatnam was called "virtuoso of the Poincaré sphere" [11] because in most of his works the Poincaré sphere plays a major role. That means to understand his ideas we have to investigate a little bit on the concept of the Poincaré sphere, which has become a powerful tool in considering polarized light [57].

The French mathematician and physicist Henry Poincaré[2] created the so called Poincaré sphere where all possible states of polarization can be depict. Each point on the sphere represents a certain state of polarization. Let us start from an general elliptical state of polarization with fixed intensity. During the propagation the vector

[1] S. Pancharatnam 1934-1969: He was 22 yeas old when he published this paper. He was an excellent physicist but he died very young at the age of 35 due to a chest illness.

[2] H. Poincaré: 1854-1912

of polarization $\vec{p}$ [3] traces out an ellipse, which can be described by two parameters (see figure 4.1(a)):

1. the azimuth angle λ, which describes the orientation of the major axis of the ellipse with respect to a fixed line

2. the ellipticity ω, which describes the ration of major a to minor b axis, $\tan\omega = \frac{b}{a}$ ranging from $-\frac{\pi}{4}$ to $+\frac{\pi}{4}$

Positive and negative values of ω represent opposite senses of polarization. A unit 2-sphere is characterized by two parameters, hence we can map the polarization states onto a unit 2-sphere such that the longitude on the sphere corresponds to 2λ and the latitude to 2ω (see figure 4.1(b)). That means all linear polarizations (such as vertical (V) or horizontal (H)) can be found on the equator. The north pole represents right handed circular (RHC) polarization and the south pole left handed circular (LHC) polarization. All points (P) in between correspond to all kinds of elliptical polarization.

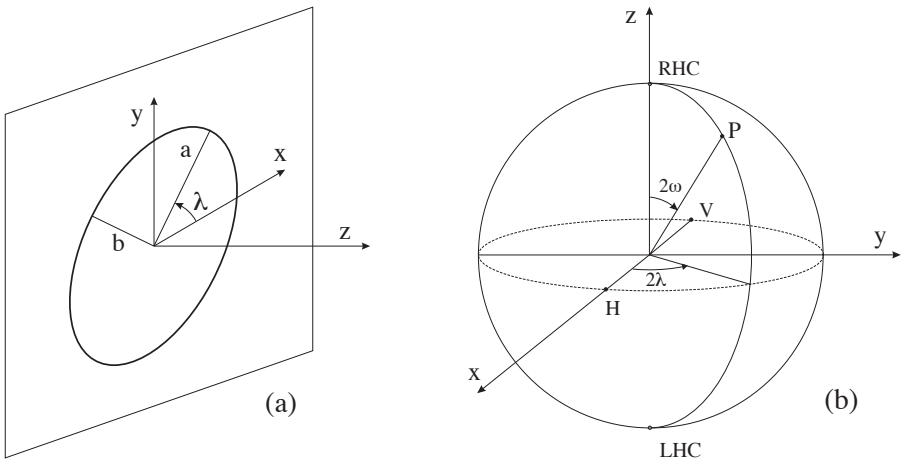

Figure 4.1: (a) General way of parameterizing an arbitrary state of polarization. (b) Poincaré sphere for all possible states of polarization.

A general intensity-preserving polarization transformation (such as half-wave-plates (HWP) or quarter-wave-plates (QWP)) are described by three parameters, the orientation of the fast axis and the angle of rotation. They are represented on the sphere by a rotation about a fixed axis through the center of the sphere (e.g. the y-axis in figure 4.1) and a certain angle of rotation (for a HWP this is π and for a QWP this is $\frac{\pi}{2}$). That means you transform for example RHC polarization by a QWP oriented along the y-axis into H polarization or with a HWP into LHC polarization.

[3] The $\vec{p}$-vector coincidences with the $\vec{E}$-vector. The plane of polarization is formed by the $\vec{B}$-vector and the $\vec{k}$-vector.

4.3 Derivation

Now we want to define the phase difference of two distinct modes of polarization in a more mathematical way than in section 4.1. Therefore we take two different normalized states named $|\psi_1\rangle$ and $|\psi_2\rangle$ which should not be orthogonal

$$\begin{aligned} \langle\psi_1|\psi_1\rangle = \langle\psi_2|\psi_2\rangle = 1 \\ \langle\psi_1|\psi_2\rangle \neq 0 \end{aligned} \tag{4.3.1}$$

Pancharatnam suggested that it is possible to compare the two states by looking at the intensity I of the superposed beam. The intensity is given by

$$I = |\ |\psi_1\rangle + |\psi_2\rangle\ |^2 = 2 + 2\Re e\big(\langle\psi_1|\psi_2\rangle\big) \tag{4.3.2}$$

The scalar product is in general a complex number and can be written in the following way

$$\langle\psi_1 \mid \psi_2\rangle = re^{i\delta} \tag{4.3.3}$$

where $r = |\langle\psi_1 \mid \psi_2\rangle|$ denotes the absolute value of the scalar product and δ is the phase. For equation (4.3.2) we only need the real part of the scalar product. Therefore we get for the intensity

$$I = 2 + 2r\cos\delta \tag{4.3.4}$$

It is senseful to interpret δ, the phase of the complex scalar product of the two states, as the phase difference. Two states are said to be in phase, if the scalar product is real and positive ($\delta = 0$) or if the intensity of the superposed beam is maximal.

The definition of two states being in phase is now to give maximum intensity in the superposition. That means in concrete: A circular and a linear polarized beam are said to be in phase if both $\vec{E}$-vectors are the same at the maximum amplitude. The same holds for elliptical and linear polarization and two elliptical or circular polarizations. Two different linear polarizations including a certain angle are in phase if the $\vec{E}$-vectors reach their maximum amplitude at the same time. This condition of being in phase can be tested in experiments very easily.

4.4 Geometrical properties

Another important point which Pancharatnam discovered was that the phase defined in equation (4.3.4) has non-transitive properties. This can be shown by the following. Suppose we have three different states $|\psi_1\rangle$, $|\psi_2\rangle$ and $|\psi_3\rangle$. We prepare them in such a way that $|\psi_1\rangle$ is in phase with $|\psi_2\rangle$ and $|\psi_2\rangle$ is in phase with $|\psi_3\rangle$. Then in general it is not the case that $|\psi_3\rangle$ is in phase with $|\psi_1\rangle$. They differ in phase by a certain amount which can be related to the solid angle they trace out on the Poincaré sphere. When we mark the states on the sphere and connect them by the great circle arcs, each less than π in extent, we get a geodesic triangle $\Delta(\psi_1, \psi_2, \psi_3)$ on the sphere (see figure 4.2).

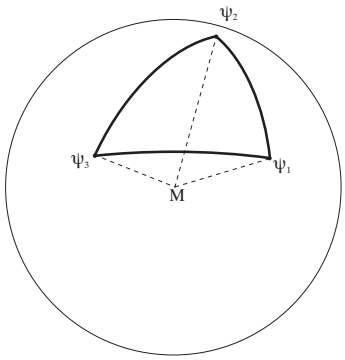

Figure 4.2: The three states forming a spherical triangle on the Poincarśphere.

The phase difference between the first and the third state is then given by

$$\delta = \frac{1}{2}\Omega_\Delta \tag{4.4.1}$$

where Ω_Δ denotes the solid angle subtended by the triangle at the origin of the sphere which is equal to the spherical excess of the triangle. This can be interpreted as a parallel transport of the polarization state on the sphere. When we subtend a closed curve the initial and the final state do not coincide in phase any more.

This phase factor also appears for nonunitary evolutions such as measurements (see for instance [6, 61]). Again we have three states $|\psi_1\rangle$, $|\psi_2\rangle$ and $|\psi_3\rangle$. A measurement can be described by a projection operator onto the eigenstate corresponding to the eigenvalue of the measured state (the outcome of the measurement). The initial state of the system is given by

$$|\psi_i\rangle = |\psi_1\rangle \tag{4.4.2}$$

Then we make the following projections: first we project onto $|\psi_2\rangle$, then onto $|\psi_3\rangle$ and finally back onto $|\psi_1\rangle$. The final state is then given by the following when we ignore the time evolution (e.g. set $H = 0$)

$$|\psi_f\rangle = |\psi_1\rangle\langle\psi_1|\psi_3\rangle\langle\psi_3|\psi_2\rangle\langle\psi_2|\psi_1\rangle \tag{4.4.3}$$

which differs from the original state $|\psi_i\rangle$ by a well-defined phase factor

$$e^{i\delta} = \langle\psi_1|\psi_3\rangle\langle\psi_3|\psi_2\rangle\langle\psi_2|\psi_1\rangle \tag{4.4.4}$$

This phase factor can be interpreted as a geometrical phase which is related to the solid angle by equation (4.4.1).

4.5 Remark

The Pancharatnam phase is said to be a noncyclic phase. This needs a little explanation, because in the above considerations we have always used closed paths. But the important fact is that the considered states were only points on the sphere.

The connecting great circle arcs were of no physical meaning. They only allowed us to interpret the occurring phase as the solid angle enclosed by the arising spherical triangle. This is in contrast to the Berry phase and the Aharonov-Anandan phase, because in these cases the system really evolves along the path C. Therefore it is justified to call these evolutions cyclical.

Chapter 5

Geometric phases in experiments

5.1 Experiments with photons

We have seen (explicitly for spin-$\frac{1}{2}$ particles, section 2.6 and 3.4) that the geometrical phase of fermions is related to the solid angle. This relation is also valid in the bosonic case. The first experiments were done with photons (spin-1 bosons) because they are rather easy to handle in experiments. There are several ways to let a photon acquire a geometrical phase.

- **Variation of propagation direction:**
  - coiled optical fibre: see section 5.1.1
  - Mach-Zehnder Interferometer: see section 5.1.2
- **Variation of polarization:** Pancharatnam phase

5.1.1 Photons in an optical fibre

This was the first experiment to confirm the prediction of Berry. In 1986 Chiao, Wu and Tomita [25, 68] devised and carried out an experiment in which the spin of photons was turned. Because the photon's spin vector points either along the direction in which it is travelling or in the opposite direction it can be easily turned by changing the direction of travel. This was done with a coiled optical fibre.

Theory

The photon is a massless spin-1 particle. Its helicity is determined by the product of the spin operator $\vec{\sigma}$ and the vector of its direction of propagation $\vec{k}$. For the helicity the following eigenvalue equation holds

$$\left(\vec{\sigma} \cdot \vec{k}\right)|k, \sigma\rangle = \sigma|k, \sigma\rangle \tag{5.1.1}$$

where the helicity eigenvalue σ is $+1$ when the spin of the photon points in the direction of propagation or -1 when the spin points in the opposite direction. It is possible to keep the helicity quantum number σ of a photon as an adiabatic invariant during the passage through an optical fibre when no reflections occur. If the fibre is wounded in such a way that the $\vec{k}$-vector traces out a closed curve, e.g. if it is helically shaped, then we can apply the concept of Berry to determine the geometrical phase acquired during the passage of the fibre. The parameterspace is the momentum space $\{\vec{k}\}$ and the adiabatic invariant property is the helicity. Berry's formula for the photon looks like the one for fermions except for a factor $\frac{1}{2}$

$$\gamma_\sigma(C) = -\sigma\Omega(C) \tag{5.1.2}$$

The solid angle $\Omega(C)$ is determined by the curve C that the $\vec{k}$-vector traces out in momentum space which can be seen in figure 5.1. We consider now linearly polarized

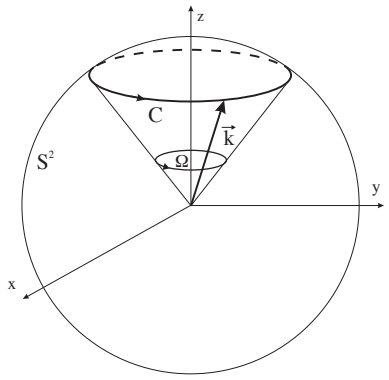

Figure 5.1: The solid angle Ω in momentum space for constant $|\vec{k}|$.

light which is a superposition of the helicity eigenstates

$$|\psi_i\rangle = \frac{1}{\sqrt{2}}\big(|k,+\rangle + |k,-\rangle\big) \tag{5.1.3}$$

After propagation through the fibre at a time T each eigenstates picks up a dynamical and a geometrical phase factor.

$$|k,\pm\rangle \longrightarrow e^{-\frac{i}{\hbar}E_\pm T} e^{i\gamma_\pm} |k,\pm\rangle \tag{5.1.4}$$

where the energy eigenvalues are taken to be time independent. The final state is then given by

$$|\psi_f\rangle = \frac{1}{\sqrt{2}}\Big(e^{-iE_+\frac{T}{\hbar}} e^{i\gamma_+}|k,+\rangle + e^{-iE_-\frac{T}{\hbar}} e^{i\gamma_-}|k,-\rangle\Big) \tag{5.1.5}$$

We can see from the definition of $\gamma_\sigma(C)$ in equation (5.1.2) that the following relation holds

$$\gamma_- = -\gamma_+ \tag{5.1.6}$$

With this equation we can compute the following transition amplitude

$$\left|\langle\psi_i|\psi_f\rangle\right|^2 = \cos^2\Big((E_- - E_+)\frac{T}{2\hbar} + \gamma_+\Big) \tag{5.1.7}$$

This cosine-term can be interpreted after Malus' law as a rotation of the plane of polarization about an angle of $\big((E_- - E_+)\frac{T}{2\hbar} + \gamma_+\big)$. That means the optical fibre, wound into a helix shaped form, leads to an effective optical activity although the material of the fibre has no optical active characteristics. (As J. A. Wheeler would say: "optical activity without optical activity") The amount of the rotation indeed does not depend on the wavelength of the light but on the solid angle and therefore on the shape of the path C of the $\vec{k}$-vector. It is a pure geometrical effect.

Experiment

For the experiment Tomita and Chiao [68] use a $s = 180$ cm long single-mode fibre which has a core diameter of 2.6 μm. The fibre is inserted into a Teflon sleeve to minimize the torsional stress which might disturb the results due to elasto-optic effects. The Teflon sleeve is helically wound onto a cylinder, which can be seen in figure 5.2. The ends of the fibre point into the same direction to ensure the closed path in $\vec{k}$-space. The polarization of the light coming from a He-Ne laser is controlled by polarizers as well as the polarization of the light leaving the fibre.

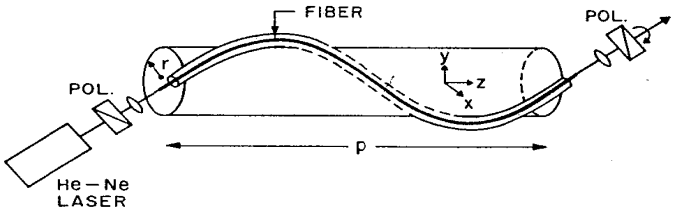

Figure 5.2: Experimental setup for Berry's phase due to a helical optical fibre. [68]

The experiment consists of two major parts. The first one is to use a fibre with constant pitch angle θ , which is defined as the angle between the local wave guide axis and the axis of the helix (see figure 5.3(a)). The pitch length p is given by

$$p = \sqrt{s^2 - (2\pi r)^2} \tag{5.1.8}$$

and is varied between 30 and 175 cm. The pitch angle is given by

$$\cos\theta = \frac{p}{s} \tag{5.1.9}$$

We get for the solid angle in $\vec{k}$-space due to the constant pitch angle

$$\Omega(C) = 2\pi(1 - \cos\theta) = 2\pi(1 - \frac{p}{s}) \tag{5.1.10}$$

which gives for the Berry phase

$$\gamma_\sigma(C) = -2\pi\sigma(1 - \frac{p}{s}) \tag{5.1.11}$$

If we assume that the two helicity eigenstates have equal energies then the calculated Berry phase (5.1.11) should be equal to the measured angle of optical polarization rotation.

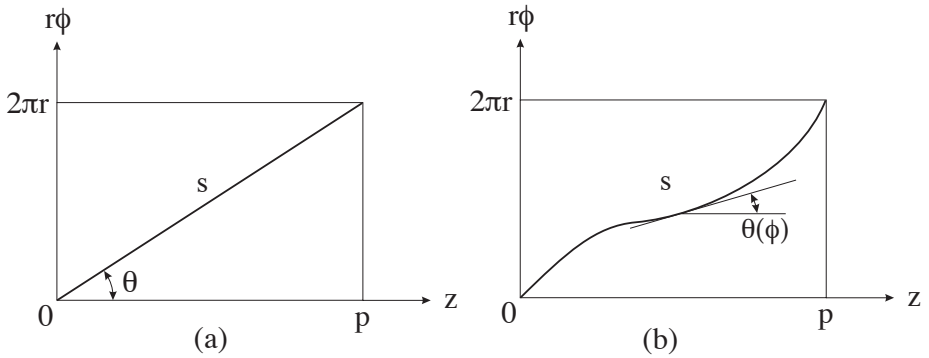

Figure 5.3: (a) Shape of the uniform wounded helical fibre. (b) Shape of the nonuniform wounded helical fibre.

For the second step of the experiment they used nonuniform wounded helical fibres (figure 5.3(b)). The curves were generated by computers and then wrapped onto the cylinder where the fibre got the same form. The pitch angle θ is variable and gets a dependency on the azimuthal angle ϕ. We get the local pitch angle by simple differentiation.

$$\tan\theta(\phi) = r\frac{d\phi}{dz} \tag{5.1.12}$$

where z represents the z-axis of the cylinder. The solid angle of the closed curve C traced out in momentum space is now given by

$$\Omega(C) = \int_0^{2\pi} \big(1 - \cos\theta(\phi)\big) d\phi \tag{5.1.13}$$

and we get for the Berry phase

$$\gamma_\sigma(C) = -\sigma\Omega(C) \tag{5.1.14}$$

which is again related to an optical rotation.

In figure 5.4 we can see the experimental measured optical rotation angles in comparison to the calculated solid angle. We see that the factor of proportion is 1, which is in agreement to the theoretical prediction. We also see that the form of the curve does not influence the Berry phase as long as the solid angle is the same which confirms the geometrical property of the phase.

5.1.2 Nonplanar Mach-Zehnder-Interferometer

The nonplanar Mach-Zehnder-Interferometer is an Interferometer which is arranged in two different plains. There were done two experiments using nonplanar Mach-Zehnder-Interferometers. We pick out the first experiment done by Chiao, Antaramian, Ganga, Jiao, Wilkinson and Nathel in 1988 [24] and describe it. The

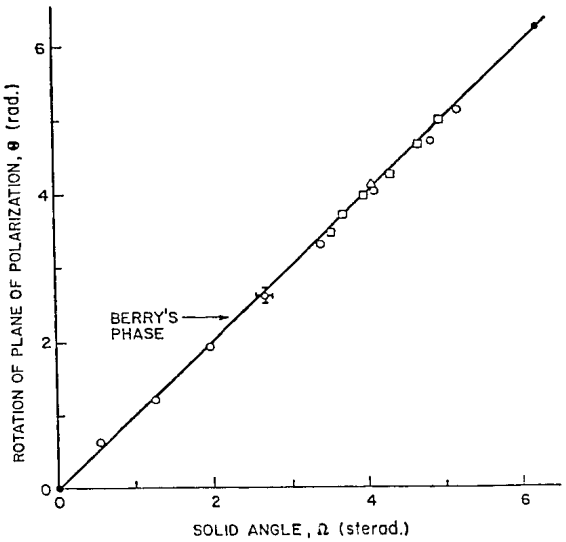

Figure 5.4: Measured angle of rotation in the fibre versus calculated solid angle: the open circle with the error bars represents the uniform helix, the other symbols represent nonuniform helixes. [68]

later experiment [40] done in 1989 uses a combination of Aharonov-Anandan and Pancharatnam phase within nearly the same experimental setup. This will not be treated here.

The experimental setup of the treated experiment [24] can be seen in figure 5.5. Because there are mirrors in the configuration which change the sign of the helicity the adiabatic condition about the invariant helicity is no more applicable. That means we have to use the construction of Aharonov and Anandan for general cyclic evolutions. The parameterspace, in this case the momentum space, is replaced by the projective Hilbertspace, which is represented here by the sphere of spin directions of the photon (see figure 5.6).

Theory

An incoming photon beam is splitted at B1 into two path. We analyze what happens to a photon travelling on path α and the same analysis holds for path β. The photon starts with an initial momentum $\vec{k}_0$ in x-direction. The spin direction is given by

$$\langle \vec{s}_0 \rangle = \vec{k}_0 = \begin{pmatrix} 1 \\ 0 \\ 0 \end{pmatrix} \tag{5.1.15}$$

After transition through B1 it has the direction $\vec{k}_1$ and a spin direction of

$$\langle \vec{s}_1 \rangle = \vec{k}_1 = \begin{pmatrix} 1 \\ 0 \\ 0 \end{pmatrix} \tag{5.1.16}$$

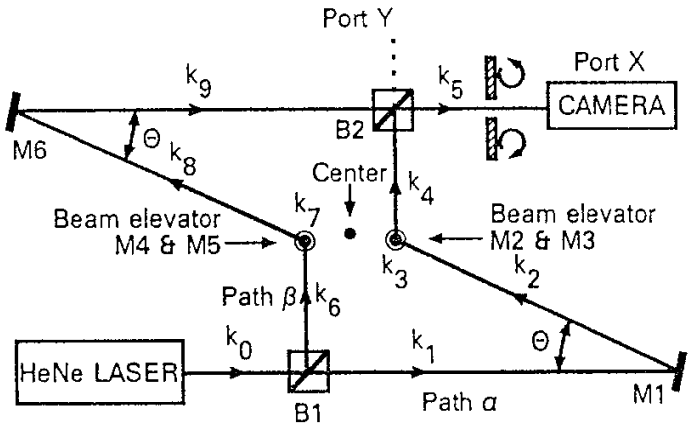

Figure 5.5: Experimental setup for the nonplanar Mach-Zehnder-Interferometer. [24]

because the sign of the helicity does not change upon transition. Then the photon is reflected at M1 into the direction $\vec{k}_2$ and due to the reflection the following spin direction

$$\langle \vec{s}_2 \rangle = -\vec{k}_2 = -\begin{pmatrix} -\cos\theta \\ \sin\theta \\ 0 \end{pmatrix} \tag{5.1.17}$$

Then the photon passes the beam elevator. This is a construction which consists of a pair of mirrors M2 and M3 which transport the beam in z-direction with momentum $\vec{k}_3$ and a spin of

$$\langle \vec{s}_3 \rangle = \vec{k}_3 = \begin{pmatrix} 0 \\ 0 \\ 1 \end{pmatrix} \tag{5.1.18}$$

At the output of the beam elevator the photon emerges along direction $\vec{k}_4$ and a spin direction of

$$\langle \vec{s}_4 \rangle = -\vec{k}_4 = -\begin{pmatrix} 0 \\ 1 \\ 0 \end{pmatrix} \tag{5.1.19}$$

When it comes to the second beam splitter B2 it is either transmitted (Y) or reflected (X) but only the reflected component at port X is detected and there the photon has a momentum of $\vec{k}_5$ corresponding to a spin direction of

$$\langle \vec{s}_5 \rangle = \vec{k}_5 = \begin{pmatrix} 1 \\ 0 \\ 0 \end{pmatrix} \tag{5.1.20}$$

We can see that the evolution is indeed a cyclic one because $\vec{k}_5 = \vec{k}_0$ and $\langle \vec{s}_5 \rangle = \langle \vec{s}_0 \rangle$. This can also be visualized by constructing the unit sphere of spin directions where the directions $\langle \vec{s}_0 \rangle$ to $\langle \vec{s}_5 \rangle$ are drawn in. They are connected by geodesics which are formed by arcs of great circles in order to give a closed curve (see figure 5.6).

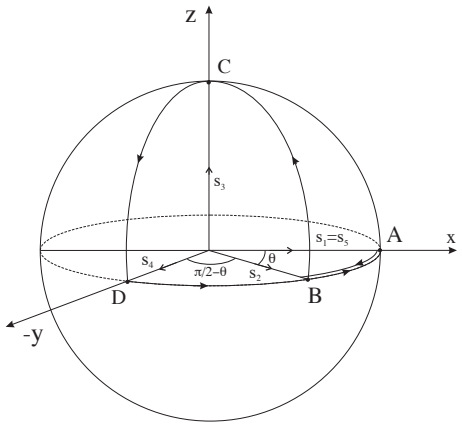

Figure 5.6: Sphere of spin directions.

We get a closed curve which is encircled by the points BCD corresponding to a solid angle. The path between A and B encloses no area. The solid angle of the curve $ABCDA$ is calculated as

$$\Omega(ABCDA) = \Omega_\alpha = \frac{\pi}{2} - \theta \tag{5.1.21}$$

The geometrical phase for path α is therefore given by

$$\beta_{\sigma,\alpha} = -\sigma\Omega_\alpha = -\sigma(\frac{\pi}{2} - \theta) \tag{5.1.22}$$

For path β the same curve on the sphere of spin directions can be used but it is traversed in the opposite direction. We get for the solid angle

$$\Omega(ADCBA) = \Omega_\beta = -\Omega_\alpha = \theta - \frac{\pi}{2} \tag{5.1.23}$$

and for the geometrical phase

$$\beta_{\sigma,\beta} = -\sigma\Omega_\beta = -\sigma(\theta - \frac{\pi}{2}) = -\beta_{\sigma,\alpha} \tag{5.1.24}$$

The two paths α and β interfere at port X where two circular polarization filters of opposite sense allow a separate detection of each sense of polarization σ. The geometrical phase changes its sign upon reversing the sense of polarization of the photon and upon the spatial inversion of the beam path, i.e the transformation of path α into path β and vice versa. The initial state is a superposition of the two helicity eigenstates

$$|\psi_i\rangle = \frac{1}{\sqrt{2}}\big(|k,+\rangle + |k,-\rangle\big) \tag{5.1.25}$$

This state picks up the respective geometrical phase and is given apart from the dynamical phase, which can be ignored because it cancels out, by

$$|\psi_f\rangle = \frac{1}{\sqrt{2}}\Big(e^{i\beta_{+,\alpha}}|k,+\rangle + e^{i\beta_{-,\alpha}}|k,-\rangle + e^{i\beta_{+,\beta}}|k,+\rangle + e^{i\beta_{-,\beta}}|k,-\rangle\Big) \tag{5.1.26}$$

We have the following phase relation for α as well as for β

$$\beta_{\sigma,\alpha} = -\beta_{-\sigma,\alpha} \tag{5.1.27}$$

We can compute the following transition amplitudes

$$\begin{aligned} \left|\langle k,+|\psi_f\rangle\right|^2 &= 2\cos^2\Big(\beta_{+,\alpha}\Big) \\ \left|\langle k,-|\psi_f\rangle\right|^2 &= 2\cos^2\Big(\beta_{-,\alpha}\Big) \end{aligned} \tag{5.1.28}$$

Therefore we get for the relative geometrical phase shift

$$2\cos^2\Big(\beta_{+,\alpha}\Big) + 2\cos^2\Big(\beta_{-,\alpha}\Big) = 4\cos^2\Big(\beta_{+,\alpha}\Big) \tag{5.1.29}$$

This means the phase shift which determines the relative phase shift of the interference fringes in the two pictures is equal to four times the geometrical phase $\beta_{+,\alpha}$. The dynamical phases cancel if the optical path lengths in both arms are equal. Therefore the interferometer has to be as symmetric as possible concerning the center of symmetry marked in figure 5.5.

Experiment

The output of the He-Ne laser is unpolarized light that means a superposition of the two helicity eigenstates. The beam splitters B1 and B2 are polarization-preserving 50%-50% cube beam splitters. All used mirrors M1-M6 are aluminized front-surface mirrors. The detection apparatus consists of a 10x beam expander followed by two circular polarization filter of opposite senses placed side by side and a camera. The filters consist of a $\lambda/4$ plate glued together with a linear polarizer. Because of the two polarizers we get two pictures, one for each sense of polarization. In figure 5.7 one such photograph for $\theta = 45°$ is shown. The fringes show a phase difference of π between left and right handed photons which is exactly 4 times the calculated geometrical phase of equation (5.1.22) which gives $\frac{\pi}{4}$.

In figure 5.8 the experimentally measured phase shifts for different values of θ (divided by 4) are plotted against the calculated values of the solid angle. We see that the theoretical predictions are confirmed up to a sign. The sign could be checked in an auxiliary experiment where a sugar solution with known optical activity was introduced into one arm of the interferometer.

5.2 Experiments with neutrons

Neutrons are fermions which are rather easy to handle because they are not sensitive to any electric fields. There are two groups of experiments with neutrons acquiring a geometric phase:

- **neutron polarimeters:** see section 5.2.1
- **neutron interferometers:** see section 5.2.2

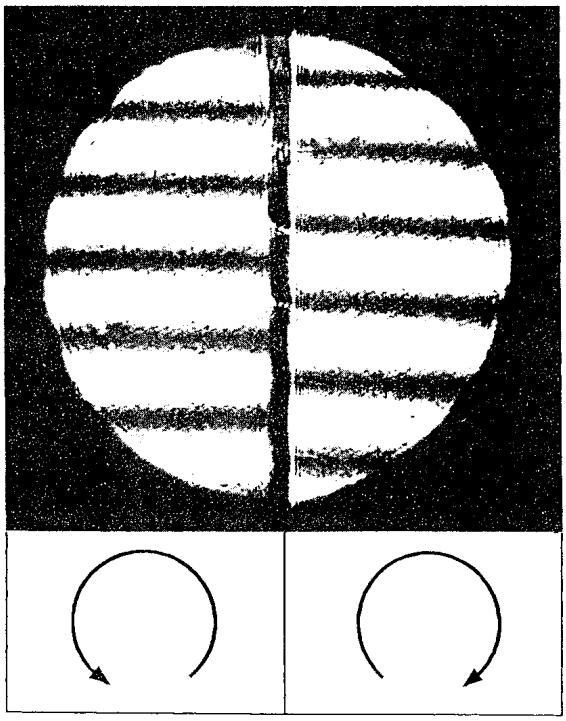

Figure 5.7: Interferogram for $\theta = 45°$. [24]

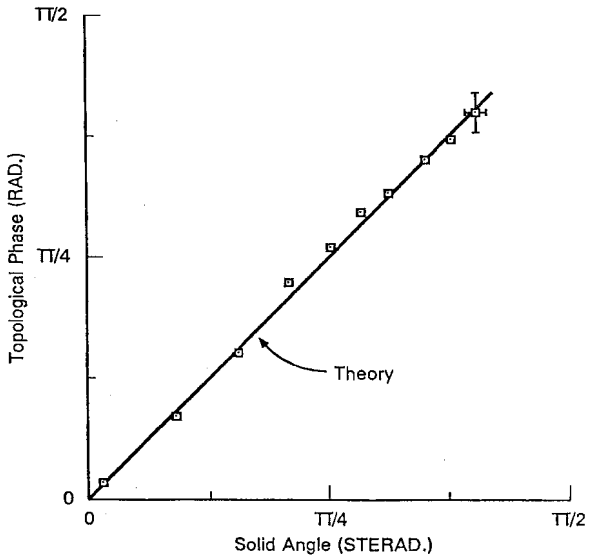

Figure 5.8: Measured geometrical phase shifts versus calculated solid angle. [24]

5.2.1 Berry phase in neutron spin rotation

The experiment of Bitter and Dubbers [18, 30] done in 1987 at the Laue-Langevin Institute in Grenoble is a polarization experiment. It was the first to show the effect of the Berry phase for fermions. The spin and the magnetic moment of the neutrons coincide therefore it is possible to turn the spin by altering the direction of an external magnetic field coupled to the magnetic moment of the neutron. In the experiment a beam of neutrons passes through a helically twisted magnetic field. This causes a geometrical phase which manifests itself in a change of the polarization of the neutrons which can be analyzed as a function of the magnetic field strength. In this experiment it is not possible to separate the geometrical phase from the dynamical one.

Theory

The neutrons pass a region with a magnetic field $\vec{B}$. The tip of the magnetic field vector follows a helical line and makes one complete turn of 2π. This field can be decomposed into a component $\vec{B}_z$ parallel to the direction of the neutron beam and an orthogonal component $\vec{B}_1$ (see figure 5.9(a)). We can introduce new variables, which denote the number of spin precessions about the various directions.

$$\begin{aligned} \zeta &= \mu B_z \frac{T}{2\pi} \\ \xi &= \mu B_1 \frac{T}{2\pi} \\ \eta &= \sqrt{\zeta^2 + \xi^2} = \mu B \frac{T}{2\pi} \end{aligned} \tag{5.2.1}$$

The total phase which is picked up during the passage is the composition of the dynamical and the geometrical phase.

$$\Phi_t = \theta + \gamma \tag{5.2.2}$$

It is now possible to calculate the total phase using standard methods (e.g. [29]), which gives

$$\Phi_t = 2\pi\sqrt{(\zeta \pm 1)^2 + \xi^2} - 2\pi \tag{5.2.3}$$

where the $\pm$ stands for right- and left-handed magnetic fields. To get a zero total phase when the field is zero we introduce the extra term of -2π. The adiabatic limit ($\eta^2 \gg \zeta$) of equation (5.2.3) gives

$$\Phi_t = 2\pi\eta - 2\pi(1 \mp \frac{\zeta}{\eta}) \tag{5.2.4}$$

When we compare this with equation (5.2.2) we can identify the first part with the dynamical phase and the second part with the geometrical phase. The geometrical phase is again connected to the solid angle in the following way

$$\gamma_\sigma = -\sigma\Omega(C) = -\sigma 2\pi(1 - \frac{\zeta}{\eta}) \tag{5.2.5}$$

where $\sigma = \pm 1$ denotes right(+)- or left(-)-handed magnetic fields. The dynamical phase stays constant during the whole experiment therefore we can ignore it in the treatise.

The experiment now measures the change of polarization between the incoming and the outgoing neutrons. When the initial polarization is denoted by $P_\alpha(0)$ and the polarization after a time T by $P_\beta(T)$ then the change of polarization can be described by a matrix equation in the following way

$$P_\beta(T) = G_{\beta\alpha}(T)P_\alpha(0) \tag{5.2.6}$$

It is possible to calculate these matrix elements $G_{\beta\alpha}$ exactly for circularly polarized fields by going to a reference system which rotates in phase with the magnetic field. We get the following formula for the zz-component

$$G_{zz}(\zeta,\xi) = \frac{(\zeta \pm 1)^2 + \xi^2 \cos(2\pi\sqrt{(\zeta \pm 1)^2 + \xi^2})}{(\zeta \pm 1)^2 + \xi^2} \tag{5.2.7}$$

This is the only component which can be derived without an ambiguity for $B_z \neq 0$. The other formulas are only valid for $B_z = 0$ and are given by

$$G_{yy}(\xi) = \cos(2\pi\sqrt{1+\xi^2}) \tag{5.2.8}$$

$$G_{zy}(\xi) = -\frac{\xi}{\sqrt{1+\xi^2}}\sin(2\pi\sqrt{1+\xi^2}) \tag{5.2.9}$$

Experiment

The neutrons have a velocity of about 500 m/s (rather slow) and a polarization of 97%. They pass a field free Mumetal cylinder with a length of 80 cm and a diameter of 30 cm which is field free. Within this cylinder there is another cylinder (length 40 cm, diameter 8 cm) where a coil is wounded on the surface to produce a static helical magnetic field $\vec{B}$. This field makes a full rotation of 2π over the length of 40 cm (see figure 5.9(b)). By another coil it is possible to produce elliptically polarized rotating fields instead of circularly polarized fields to change the specific form of the path C the magnetic field traces out. The direction of the polarization of the entering neutrons can be chosen arbitrarily as well as the analyzed component after the passage. There is no loss of polarization during the passage through the cylinder. The neutrons non-adiabatically enter the region with the magnetic field, during the passage the field turns them adiabatically and afterwards they travel of again non-adiabatically.

Measurements were made of G_{zz} as a function of B_1 and B_z and of G_{xx}, G_{yy}, G_{zx}, G_{zy} as functions of B_1 with $B_z = 0$. Figure 5.10(a) shows one such measurement of G_{yy} with $B_z = 0$ which is fitted by equation (5.2.8). Without a twisted magnetic field, that means when the geometrical phase is zero, this figure would show a simple cosine-function because then $(1 + \xi^2)$ has to be replaced by ξ^2. In figure 5.10(b) we can see the measured and the calculated total phase shift. The measured values asymptotically reach the predicted values. The jump at the origin can be explained because when the field vanishes the dynamical phase should also vanish

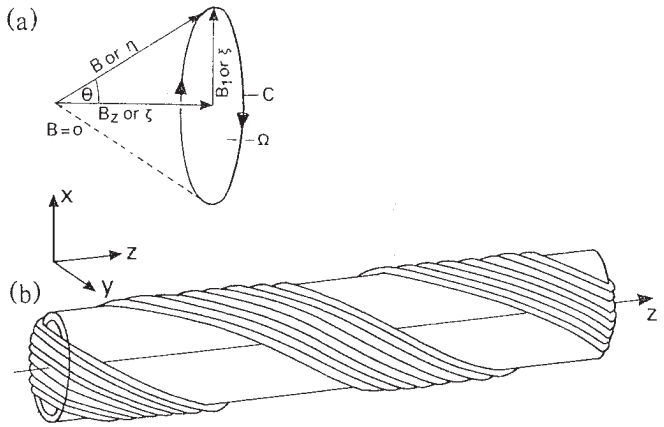

Figure 5.9: (a) Magnetic field vector tracing out a closed loop C. (b) Experimental setup for the neutron spin rotation experiment with a helically wounded coil. The neutron beam is along the z-direction. [18]

and leave only the geometrical phase. But in this experiment it is not possible to clearly separate both parts and therefore the dynamical phase dominates and sets the whole phase to zero.

Figure 5.11 shows Berry's phase as a function of the ratio $\frac{B_z}{B_1} = \frac{\zeta}{\xi}$. For this figure measurements of $G_{zz}(\zeta)$ at a fixed value of ξ are used. This corresponds to various opening angles of the magnetic field. The solid angle is drawn into the figure according to the formula

$$\Omega = 2\,\pi(1 - \frac{\zeta}{\eta}) = 2\pi(1 - \frac{B_z}{B}) \tag{5.2.10}$$

This shows the dependence of the Berry phase on the solid angle and therefore its geometrical property but not very clearly.

5.2.2 Geometric phase in coupled neutron interference loops

In 1996 Hasegawa, Zawisky, Rauch and Ioffe [39] did an interesting interferometer experiment with neutrons. They use a two loop neutron interferometer (see figure 5.12) which consists of loop A, where the geometric phase is generated, and loop B, which is a reference beam for the measurement of the phase. Various geometric phases can be generated by different combinations of a phase shifters (PS I) and an absorber. Another phase shifter (PS II) in Loop B allows to measure the geometrical phase shift. In this experiment it is possible to get rid of the dynamical phase by a certain choice of the experimental setup.

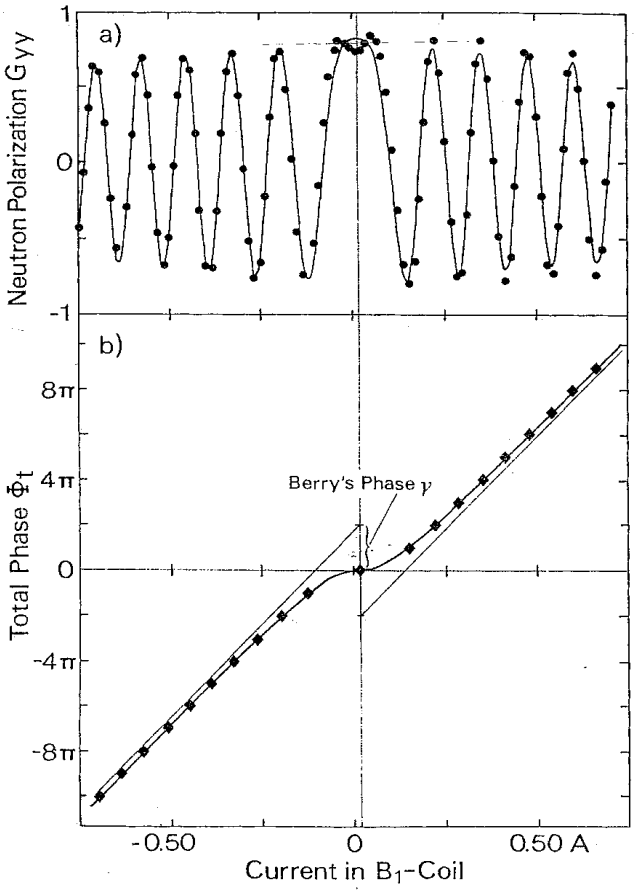

Figure 5.10: (a) Neutron spin-rotation pattern for the matrix element G_{yy}. (b) Observed and calculated total phase shift. [18]

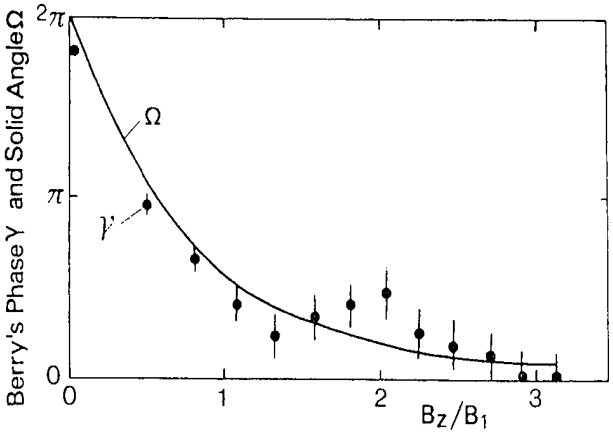

Figure 5.11: Berry phase γ and solid angle Ω for the neutron spin-rotation experiment. [18]

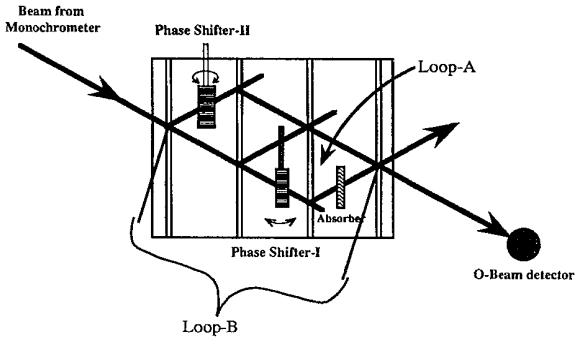

Figure 5.12: Experimental setup for the two loop neutron interferometer. [39]

Theory

It is useful to compare the interferometer with a spin-$\frac{1}{2}$ system. The two basis states "up" and "down" are identified with the two possible paths in the interferometer. In each path the neutron gets a certain phase shift χ_i. The recombined beam is said to be in phase with the initial one if the total phase shift is an integer multiple of 2π

$$\chi_I - \chi_{II} = 2n\pi \tag{5.2.11}$$

This gives the cyclicity condition for the system.

The dynamical and the geometrical phase are defined in total analogy to the spin-$\frac{1}{2}$ case. We get for the dynamical phase

$$\theta(T) = -\frac{1}{\hbar}\int_0^T \langle\psi(t)|H(t)|\psi(t)\rangle dt = \frac{1}{1+T}\big(\chi_I + T\chi_{II}\big) \tag{5.2.12}$$

The geometrical phase is given by

$$\beta(T) = \phi(T) - \theta(T) \tag{5.2.13}$$

where $\phi(T)$ is the total phase shift during the cyclic evolution. To observe only the geometrical phase one has to set the change of the dynamical phase to zero. This is assured by the following condition

$$\Delta\chi_I + T\Delta\chi_{II} = 0 \tag{5.2.14}$$

where $\Delta\chi_i$ stands for the change of phase in the i^{th} path and T is the transmission probability of the absorber in path II. Then the observed total phase shift is equal to the geometrical phase shift.

It is possible to construct a Poincaré sphere for this problem (see figure 5.13). The vertical axis represent the relative intensity of the two beams, where the polar points stand for the single beam situation. This can be varied by the transmission probability T. The horizontal axis represents the relative phase between the two beams. In the cyclic case this angle is varied from 0 to 2π. This means for a certain

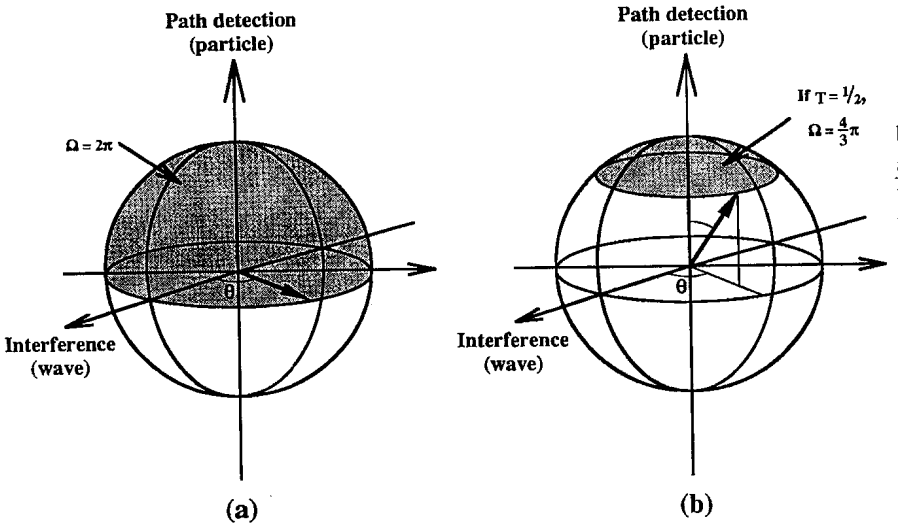

Figure 5.13: (a) Poincaré sphere for $T = 1$. (b) Poincaré sphere for $T = \frac{1}{2}$. [39]

type of absorber with fixed transmission possibility T that the state traces out a latitudinal circle on the sphere. We can define the solid angle for this evolution as the part of the sphere which lies above the latitudinal circle. The solid angle is then given by

$$\Omega(C) = 4\pi \frac{T}{1+T} \tag{5.2.15}$$

The Berry phase expressed in terms of the solid angle is then given by

$$\beta(C) = \sigma\Omega(C) = 4\pi\sigma \frac{T}{1+T} \tag{5.2.16}$$

where σ is some constant called helicity which has to be specified by the experiment. The geometrical phase depends only on the transmission probability T of the absorber and determines the path on the Poincaré sphere.

Experiment

The experiment was done at the neutron interferometer instrument V9 at the BENSC Hahn-Meitner-Institute in Berlin. The four-plate neutron interferometer is made out of a monolithic perfect silicon crystal. The neutron beam's wavelength is 1.95 Åand has a cross section of 2 mm (horizontal) and 10 mm (vertical). The O-beam is detected by a He-3 detector which has a typical counting rate of 0.627(8) per second.

They investigates on three different experimental setups to produce Berry phases characterized by

1. (a) no absorber, which gave $T = 1$
2. (b) absorber A (1 mm gold foil) with $T = 0.493(14)$

3. (c) absorber B (1 mm gold foil and 1 mm indium foil) with $T = 0.212(15)$

The phase shifters are made out of parallel-sided aluminium plates which have different thicknesses according to the used absorber to fulfill equation (5.2.14) for zero dynamical phase. The used combinations are listed in the following.

	Absorber	thickness of PS in path I	thickness of PS in path II
(a)	no	5 mm	5 mm
(b)	absorber A	5 mm	10 mm
(c)	absorber B	2 mm	10 mm

When the Al-plates are a little rotated around the vertical axis they produce a variable phase shift due to their variable thickness according to

$$\Delta\chi_i = -N\lambda b_c \Delta D_i \tag{5.2.17}$$

where N is the number of nuclei per volume, λ is the wavelength of the neutrons, b_c is the coherent scattering length of aluminium and ΔD_i is the Change in thickness of the plate.

The experiment was done in two steps. First loop B was blocked to test out the different combinations of absorbers and phase shifters. The results are shown in figure 5.14 where only the combinations (a) and (b) are presented. We can see a reduction in the amplitude due to the decreasing transmission probability.

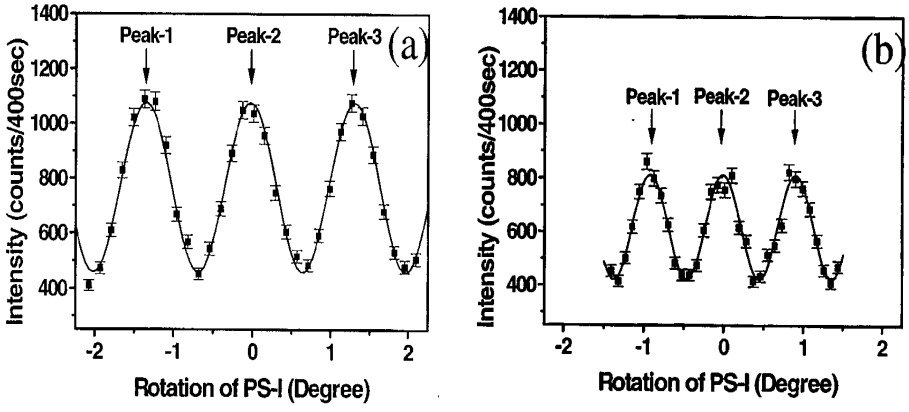

Figure 5.14: Results for the case (a) and (b) when loop B is blocked. [39]

The second step is to unblocked loop B. PS I is set at each of the maximums (peak-1, peak-2 and peak-3) of the oscillations from figure 5.14. By rotations of PS II (5 mm thick) intensity modulations were produced (see figure (5.15)). The measurements were taken again for each combination (a)-(c) of absorber and PS I.

When we compare the modulations of the various peaks for a fixed case (a), (b) or (c) we see a clear phase shift between the fringe patterns. This phase shifts can be determined from the experimental data and compared with the theoretical predictions. The experimental determined value of $\beta(C)$ and the theoretical values of $\Omega(C)$ according to equation (5.2.15) are shown in the following table

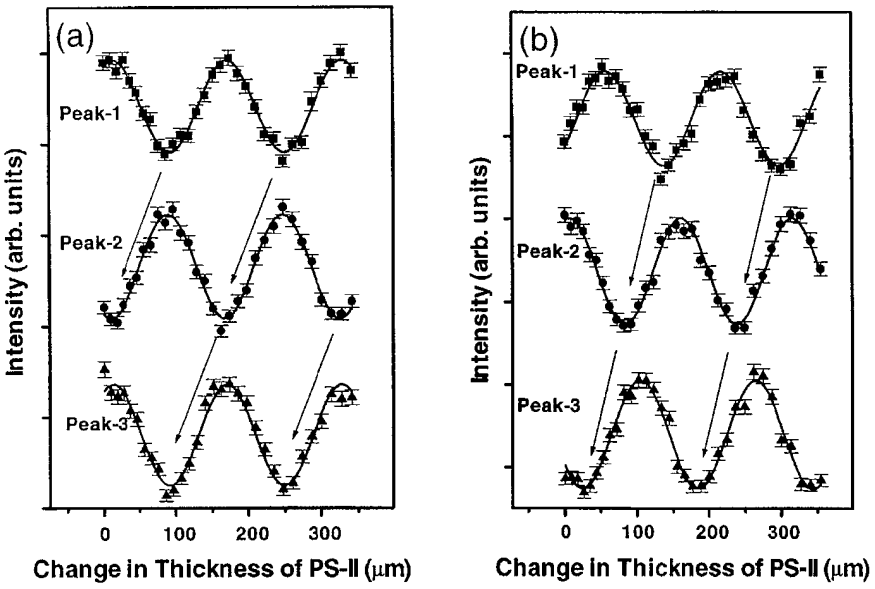

Figure 5.15: Intensity modulations due to PS II for (a) and (b). [39]

case	theoretical value of $\Omega(C)$	experimental value of $\beta(C)$
(a)	2π	3.144±0.038
(b)	4.150	2.207±0.054
(c)	2.198	1.222±0.060

This fits very good when we set the free parameter $\sigma = \frac{1}{2}$. The data are plotted in figure 5.16 and confirm the statement that the measured phase is a geometrical one.

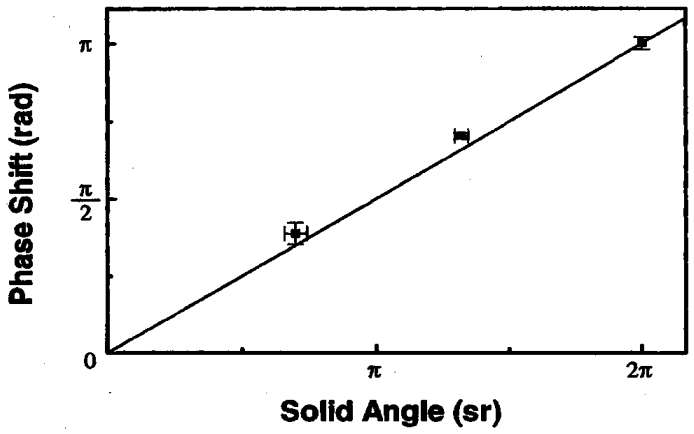

Figure 5.16: Measured phase shift β versus calculated solid angle Ω. [39]

5.3 List of further experiments

There have been many other experiments observing Berry's phase. Here we give a short overview.

Photons:
- 1988 Pancharatnam phase by Bhandari, Samuel, Chyba, Wang, Mandel and Simon [16, 17, 26]
- 1988 time reversal of geometrical phase by Tompkin, Malcuit, Boyd and Chiao [69]
- 1988 geometrical phase as frequency shift by Simon, Kimble and Sudarshan [65]
- 1989 Berry and Pancharatnam phase by Jiao, Wilkinson, Chiao and Nathel [40]
- 1991 nonclassical Berry phase by Kwiat and Chiao [43]

Neutrons:
- 1988 with ultracold neutrons by Richardson, Kilvington, Green and Lamoreaux [59]
- 1990 noncyclic evolution with polarimeter by Weinfurter and Badurek [79]
- 1997 separation of dynamical and geometrical phase by Wagh, Rakhecha, Summhammer, Badurek, Weinfurter, Allman, Kaiser Hamacher, Jacobson and Werner [73]
- 1998 noncyclic evolution with interferometer by Wagh, Rakhecha, Fischer and Ioffe [72]
- 2000 neutron polarimeter by Wagh, Badurek, Rakhecha, Buchelt and Schricker [71]
- 2001 off-diagonal geometric phase by Hasegawa, Loidl, Baron, Badurek and Rauch [38]

Atomic Na_3 clusters 1986 by Delacretaz, Grant, Whetten, Wöste and Zwanziger [28]

Nuclear magnetic resonance: 1987 by Suter, Chingas, Harris and Pines [66]

Nuclear quadrupole resonance: 1987 by Tycko [70]

Atom interferometer: 1999 by Webb, Godun, Summy, Oberthaler, Featonby, Foot and Burnett [78]

This list is not complete but it gives an idea how much different applications and approaches there are for the geometrical phase.

Chapter 6

Applications

6.1 Berry phase in entangled systems

6.1.1 Introduction

In 1935 Schrödinger [62] denoted entanglement as a fundamental concept of Quantum mechanics. Einstein pointed out that superpositions can lead to paradoxical quantum nonlocality. The problem was formulated in the famous gedanken experiment published together with Podolsky and Rosen [32]. They concluded form nonlocality that quantum mechanics cannot be complete and must be modified by some "hidden variables". The following debate was put on an objective level by John Bell in 1964 [5]. He derived an inequality based on hidden variable theory for joined measurement probabilities for entangled systems. The version published by Clauser, Horne, Shimony and Holt (CHSH) [27] allowed an experimental decision between hidden variable theories and quantum mechanics. Experiments on this subject were done mostly with photons but also with massive systems, e.g. neutral kaons [14, 15]. So far all experiments confirm that they are not compatible with any hidden variable theory. The violation of Bell's inequality confirms that quantum mechanic is a nonlocal theory.

The experiments described in section 5.1 can also be understood with classical Maxwell equations. This was long time a point of critics, because Berry proposed a quantal phase factor. In 1991 Kwiat and Chiao [43] did an experiment with entangled photons, where the quantal character of the phase was confirmed.

In a recent work [13] the concepts of Berry phase and entanglement are worked out in more detailed way. The authors establish Bell inequalities, which can be violated by variable Berry phases.

6.1.2 Bell inequality

We consider a pair of entangled spin-$\frac{1}{2}$ particles produced in a spin singlet state

$$|\psi\rangle = \frac{1}{\sqrt{2}}\Big\{ |\Uparrow\rangle_l \otimes |\Downarrow\rangle_r - |\Downarrow\rangle_l \otimes |\Uparrow\rangle_r \Big\} \tag{6.1.1}$$

where l and r denotes left and right side[1] and the spin eigenstates are taken with respect to the z-axis. We measure on the left side the spin at an angle α from an arbitrary defined measurement-axis $\vec{n}$ and on the right side at an angle β. The probability of finding on the left side, for instance, spin-up and on the right side spin-up is given by

$$\begin{aligned} &P(\alpha \Uparrow_n, \beta \Uparrow_n) \\ &\quad = \left\| \left(\langle \Uparrow_n | \cos\frac{\alpha}{2} + \langle \Downarrow_n | \sin\frac{\alpha}{2} \right) \otimes \left(\langle \Uparrow_n | \cos\frac{\beta}{2} + \langle \Downarrow_n | \sin\frac{\beta}{2} \right) |\psi\rangle \right\|^2 \\ &\quad = \frac{1}{2}\sin^2\frac{\alpha-\beta}{2} \end{aligned} \tag{6.1.2}$$

and to find on the left side spin up and on the right side spin down is given by

$$\begin{aligned} &P(\alpha \Uparrow_n, \beta \Downarrow_n) \\ &\quad = \left\| \left(\langle \Uparrow_n | \cos\frac{\alpha}{2} + \langle \Downarrow_n | \sin\frac{\alpha}{2} \right) \otimes \left(-\langle \Uparrow_n | \sin\frac{\beta}{2} + \langle \Downarrow_n | \cos\frac{\beta}{2} \right) |\psi\rangle \right\|^2 \\ &\quad = \frac{1}{2}\cos^2\frac{\alpha-\beta}{2} \end{aligned} \tag{6.1.3}$$

The expectation value for a given angle combination derives to

$$\begin{aligned} E(\alpha,\beta;n) &= P(\alpha \Uparrow_n, \beta \Uparrow_n) + P(\alpha \Downarrow_n, \beta \Downarrow_n) - P(\alpha \Uparrow_n, \beta \Downarrow_n) - P(\alpha \Downarrow_n, \beta \Uparrow_n) \\ &= -\cos(\alpha-\beta) \end{aligned} \tag{6.1.4}$$

We can combine several expectation values and get a function named S

$$S(\alpha,\beta,\gamma,\delta) = |E(\alpha,\beta;n,n') - E(\alpha,\gamma;n,n')| + |E(\delta,\beta;n,n') + E(\delta,\gamma;n,n')| \tag{6.1.5}$$

The CHSH inequality, which is a special Bell inequality, is then given by

$$S(\alpha,\beta,\gamma,\delta) \;\leq\; 2 \tag{6.1.6}$$

which is maximally violated by the quantum mechanical expectation values for the following angles

$$S^{QM}(0, \frac{\pi}{4}, \frac{3\pi}{4}, \frac{\pi}{2}) = 2\sqrt{2} \not\leq 2 \tag{6.1.7}$$

6.1.3 Berry phase and the entangled system

Berry phase on one particle of an EPR-pair

We modify the initial state by applying a Berry phase on the left moving particle. The geometrical phase can be achieved for instance by an interaction of the particle with an external magnetic field that rotates at an angle ϑ around the z-axes, as described in section 2.6.

[1] In the following we suppress the indices l and r.

We start with the initial state

$$|\psi(t=0)\rangle = \frac{1}{\sqrt{2}}\Big\{ |\Uparrow\rangle \otimes |\Downarrow\rangle - |\Downarrow\rangle \otimes |\Uparrow\rangle \Big\} \tag{6.1.8}$$

The magnetic field vector $\vec{B}(t=0=T)$ points into the direction $\vec{n}$ when the left particle enters, respectively leaves (see figure 6.1).

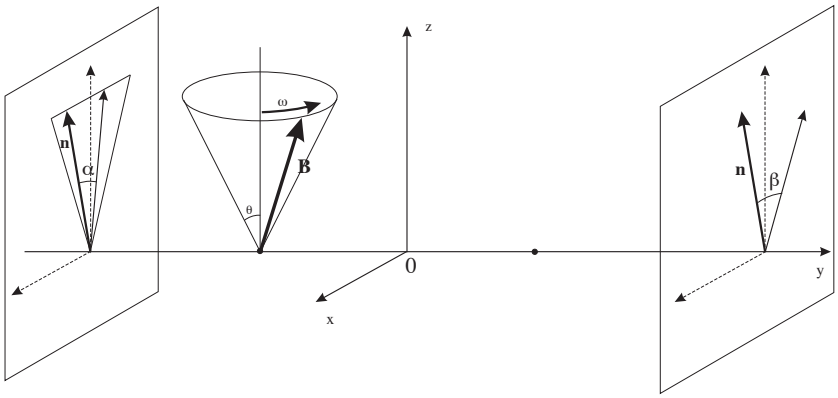

Figure 6.1: Berry phase on the left particles of the EPR-pair: the measurement can be interpreted as a projection onto the xz-plane.

The initial state picks up a dynamical and a geometrical phase which modifies the state in the following way

$$\begin{aligned} |\psi(t=T)\rangle = \frac{1}{\sqrt{2}}\Big\{ & e^{i\gamma_+(\vartheta)}\, e^{i\theta_+(T)} \mid \Uparrow_n\rangle \otimes |\Downarrow_n\rangle \\ & - e^{i\gamma_-(\vartheta)}\, e^{i\theta_-(T)} \mid \Downarrow_n\rangle \otimes |\Uparrow_n\rangle \Big\} \end{aligned} \tag{6.1.9}$$

where $\theta_\pm(T) = \mp\frac{\mu}{\hbar}B_0 T$ denotes the dynamical phase and $\gamma_\pm(\vartheta) = -\pi(1 \mp \cos\vartheta)$ denotes the Berry phase. We can rewrite this state by neglecting an overall phase factor

$$|\psi(t=T)\rangle = \frac{1}{\sqrt{2}}\Big\{ |\Uparrow_n\rangle \otimes |\Downarrow_n\rangle - e^{i\phi(\vartheta)} |\Downarrow_n\rangle \otimes |\Uparrow_n\rangle \Big\} \tag{6.1.10}$$

where $\phi(\vartheta) = \gamma_-(\vartheta) - \gamma_+(\vartheta) + \theta_-(T) - \theta_+(T) = 2\gamma_-(\vartheta) + 2\theta_-(T)$. The probabilities of finding spin-upon the left side under an angle α from the measurement axis $\vec{n}$ and spin-up on the right side under an angle β can be calculated analog to the last section. This gives

$$\begin{aligned} P(\alpha \Uparrow_n, \beta \Uparrow_n) &= \frac{1}{2}\left| \cos\frac{\alpha}{2}\sin\frac{\beta}{2} - e^{i\phi(\vartheta)}\ \sin\frac{\alpha}{2}\cos\frac{\beta}{2} \right|^2 \\ &= \frac{1}{2}\sin^2\frac{\alpha-\beta}{2} + (1-\cos\phi(\vartheta))\ \ \frac{\sin\alpha\cdot\sin\beta}{4} \end{aligned} \tag{6.1.11}$$

and for spin-up on the left side and spin-down on the right side

$$\begin{aligned} P(\alpha \Uparrow_n, \beta \Downarrow_n) &= \frac{1}{2}\left|\cos\frac{\alpha}{2}\sin\frac{\beta}{2} - e^{i\phi(\vartheta)}\ \sin\frac{\alpha}{2}\cos\frac{\beta}{2}\right|^2 \\ &= \frac{1}{2}\cos^2\frac{\alpha-\beta}{2} + (1-\cos\phi(\vartheta))\ \ \frac{\sin\alpha\cdot\sin\beta}{4} \end{aligned} \tag{6.1.12}$$

We calculate the expectation value as it is given by equation (6.1.4)

$$E(\alpha,\beta;n) = -\cos(\alpha-\beta) + (1-\cos\phi(\vartheta))\ \sin\alpha\cdot\sin\beta \tag{6.1.13}$$

In comparison with the result of the last section we notice an additional phase-dependent term. The only problem is that the phase $\phi(\vartheta)$ also has dynamical components in it and the effect of the geometrical phase is suppressed by the dynamical phase. In this setup we are not sensitive to the Berry phase[2].

Berry phase on both particles of the EPR-pair

We investigate on the case where both particles enter an external magnetic field, which has the same absolute value B_0. The field precesses with the same frequency ω around the z-axis but the apex angles ϑ and ϑ' on both sides are different (see figure 6.2).

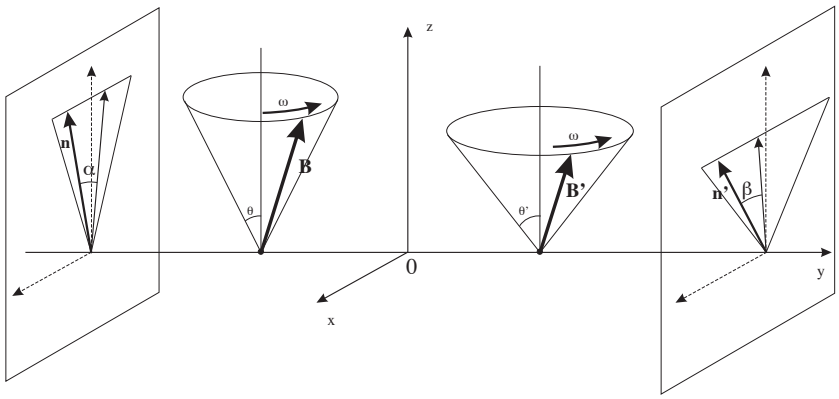

Figure 6.2: Berry phase on both particles of the EPR-pair: the measurement can be interpreted as a projection onto the xz-plane.

In this case it is also important where the field starts its circular motion. This is parameterized by additional angles α_0 and α_0' which are measured from a reference axis, for instance the x-axis. We get the following magnetic fields

$$\vec{B}(t) = B_0\begin{pmatrix}\sin\vartheta\cos(\omega t+\alpha_0)\\ \sin\vartheta\sin(\omega t+\alpha_0)\\ \cos\vartheta\end{pmatrix} \qquad \vec{B}'(t) = B_0\begin{pmatrix}\sin\vartheta'\cos(\omega t+\alpha_0')\\ \sin\vartheta'\sin(\omega t+\alpha_0')\\ \cos\vartheta'\end{pmatrix} \tag{6.1.14}$$

[2]This is in contrast to reference [43], where the expectation values depend on the geometrical phase but in our case they depend on the cosine of the phase.

The procedure of creating a geometrical phase is the same as described above. The initial state is a spin-singlet state produced by a source in the z-basis

$$|\psi(t=0)\rangle_{z,z} = \frac{1}{\sqrt{2}}\left\{|\Uparrow_z\rangle \otimes |\Downarrow_z\rangle - |\Downarrow_z\rangle \otimes |\Uparrow_z\rangle\right\} \tag{6.1.15}$$

Now we express this spin-singlet state in the n-basis[3] because this makes calculations easier. The basis vectors in z expressed in n are given by

$$\begin{aligned} |\Uparrow_z\rangle &= \quad \cos\frac{\vartheta}{2}|\Uparrow_n\rangle + \sin\frac{\vartheta}{2}e^{i\alpha_0}|\Downarrow_n\rangle \\ |\Downarrow_z\rangle &= -\sin\frac{\vartheta}{2}|\Uparrow_n\rangle + \cos\frac{\vartheta}{2}e^{i\alpha_0}|\Downarrow_n\rangle \end{aligned} \tag{6.1.16}$$

Inserting equation (6.1.16) into equation (6.1.15) we get the following state, where an overall phase factor $e^{-i\alpha_0}$ has been taken out and ignored.

$$\begin{aligned} |\psi(t=0)\rangle_{n,n'} = \frac{1}{\sqrt{2}}\{&a_1|\Uparrow_n\rangle \otimes |\Uparrow_{n'}\rangle + a_2|\Downarrow_n\rangle \otimes |\Downarrow_{n'}\rangle \\ &+ a_3|\Uparrow_n\rangle \otimes |\Downarrow_{n'}\rangle + a_4|\Downarrow_n\rangle \otimes |\Uparrow_{n'}\rangle\} \end{aligned} \tag{6.1.17}$$

The coefficients are given by

$$\begin{aligned} a_1 &= \quad \cos\frac{\vartheta}{2}\sin\frac{\vartheta'}{2} - e^{i\Delta\alpha_0}\sin\frac{\vartheta}{2}\cos\frac{\vartheta'}{2} \\ a_2 &= -\sin\frac{\vartheta}{2}\cos\frac{\vartheta'}{2} + e^{i\Delta\alpha_0}\cos\frac{\vartheta}{2}\sin\frac{\vartheta'}{2} \\ a_3 &= \quad \cos\frac{\vartheta}{2}\cos\frac{\vartheta'}{2} + e^{i\Delta\alpha_0}\sin\frac{\vartheta}{2}\sin\frac{\vartheta'}{2} \\ a_4 &= -\sin\frac{\vartheta}{2}\sin\frac{\vartheta'}{2} - e^{i\Delta\alpha_0}\cos\frac{\vartheta}{2}\cos\frac{\vartheta'}{2} \end{aligned} \tag{6.1.18}$$

where $\Delta\alpha_0 = \alpha_0 - \alpha_0'$. After the interaction of both particles with the external fields we get the following state

$$\begin{aligned} |\psi(t=T)\rangle_{n,n'} = \frac{1}{\sqrt{2}}\Big\{ &a_1 \cdot e^{i(\gamma_+(\vartheta)+\gamma_+(\vartheta'))}\, e^{2i\theta_+(T)}|\Uparrow_n\rangle \otimes |\Uparrow_{n'}\rangle \\ &+a_2 \cdot e^{i(\gamma_-(\vartheta)+\gamma_-(\vartheta'))}\, e^{2i\theta_-(T)}|\Downarrow_n\rangle \otimes |\Downarrow_{n'}\rangle \\ &+a_3 \cdot e^{i(\gamma_+(\vartheta)+\gamma_-(\vartheta'))}|\Uparrow_n\rangle \otimes |\Downarrow_{n'}\rangle \\ &+a_4 \cdot e^{i(\gamma_-(\vartheta)+\gamma_+(\vartheta'))}|\Downarrow_n\rangle \otimes |\Uparrow_{n'}\rangle\Big\} \end{aligned} \tag{6.1.19}$$

Here the dynamical phase cancels only for the off-diagonal spin combination (spin-up, spin-down and spin-down, spin-up) but remains for the diagonal combination (spin-up, spin-up and spin-down, spin-down) combinations. To get rid of the remaining dynamical phases we have to apply a trick. In the so called spin-echo technique the same procedure with the magnetic field is done again but with rotation in the

[3]The vector $\vec{n}$ points into the direction of the magnetic field $\vec{B}$.

reversed direction. This gives the same Berry phase as before but the dynamical phase gets a minus sign. This kills the dynamical phase also for the diagonal terms. We get for the final state

$$\begin{aligned}|\psi(t=2T)\rangle_{n,n'} = \frac{1}{\sqrt{2}}\Big\{ & a_1 \cdot e^{2i(\gamma_+(\vartheta)+\gamma_+(\vartheta'))}|\Uparrow_n\rangle \otimes |\Uparrow_{n'}\rangle \\ & +a_2 \cdot e^{2i(\gamma_-(\vartheta)+\gamma_-(\vartheta'))}|\Downarrow_n\rangle \otimes |\Downarrow_{n'}\rangle \\ & +a_3 \cdot e^{2i(\gamma_+(\vartheta)+\gamma_-(\vartheta'))}|\Uparrow_n\rangle \otimes |\Downarrow_{n'}\rangle \\ & +a_4 \cdot e^{2i(\gamma_-(\vartheta)+\gamma_+(\vartheta'))}|\Downarrow_n\rangle \otimes |\Uparrow_{n'}\rangle \Big\}\end{aligned} \tag{6.1.20}$$

With this final state vector we can calculate the probability for finding under an angle α from the quantization axis $\vec{n}$ spin up and under an angle β from the quantization axis $\vec{n}'$ also spins up

$$\begin{aligned}P(\alpha \Uparrow_n, \beta \Uparrow_{n'}) = \Big\| \frac{1}{\sqrt{2}}\Big(& a_1\, e^{2i(\gamma_+(\vartheta)+\gamma_+(\vartheta'))} \cos\frac{\alpha}{2}\cos\frac{\beta}{2} \\ & +a_2\, e^{2i(\gamma_-(\vartheta)+\gamma_-(\vartheta'))} \sin\frac{\alpha}{2}\sin\frac{\beta}{2} \\ & +a_3\, e^{2i(\gamma_+(\vartheta)+\gamma_-(\vartheta'))} \cos\frac{\alpha}{2}\sin\frac{\beta}{2} \\ & +a_4\, e^{2i(\gamma_-(\vartheta)+\gamma_+(\vartheta'))} \sin\frac{\alpha}{2}\cos\frac{\beta}{2}\Big)\Big\|^2\end{aligned} \tag{6.1.21}$$

This gives after some calculation the following probability. We have used that $|a_1|^2 = |a_2|^2$ and $|a_1|^3 = |a_4|^2$ and we introduced $\Delta\gamma(\vartheta) = \gamma_+(\vartheta) - \gamma_-(\vartheta)$. This gives the following

$$\begin{aligned}&P(\alpha \Uparrow_n,\beta \Uparrow_{n'}) = \\ &\frac{1}{8}\Big\{ \Big(1 - \cos\vartheta\cos\vartheta' - \sin\vartheta\sin\vartheta'\cos(\Delta\alpha_0)\Big)(1+\cos\alpha\cos\beta) \\ &+\Big(1 + \cos\vartheta\cos\vartheta' + \sin\vartheta\sin\vartheta'\cos(\Delta\alpha_0)\Big)(1-\cos\alpha\cos\beta) \\ &+\Big\{ (\cos(\Delta\alpha_0)(1-\cos\vartheta\cos\vartheta') - \sin\vartheta\sin\vartheta')\cos(2(\Delta\gamma(\vartheta)+\Delta\gamma(\vartheta')))\sin\alpha\sin\beta \\ &\quad + (-\cos(\Delta\alpha_0)\sin\vartheta\cos\vartheta' + \cos\vartheta\sin\vartheta')\cos(2(\Delta\gamma(\vartheta')))(1+\cos\alpha)\sin\beta \\ &\quad + (-\cos(\Delta\alpha_0)\cos\vartheta\sin\vartheta' + \sin\vartheta\cos\vartheta')\cos(2(\Delta\gamma(\vartheta)))\sin\alpha(1+\cos\beta) \\ &\quad + (\cos(\Delta\alpha_0)\cos\vartheta\sin\vartheta' - \sin\vartheta\cos\vartheta')\cos(2(\Delta\gamma(\vartheta)))\sin\alpha(1-\cos\beta) \\ &\quad + (\cos(\Delta\alpha_0)\sin\vartheta\cos\vartheta' - \cos\vartheta\sin\vartheta')\cos(2(\Delta\gamma(\vartheta')))(1-\cos\alpha)\sin\beta \\ &\quad + (-\cos(\Delta\alpha_0)(1+\cos\vartheta\cos\vartheta') - \sin\vartheta\sin\vartheta')\cos(2(\Delta\gamma(\vartheta)-\Delta\gamma(\vartheta')))\sin\alpha\sin\beta\Big\}\Big\}\end{aligned} \tag{6.1.22}$$

This formula looks rather complicated, but when we make the simplification that

$\Delta\alpha_0 = 0$, we get the following result

$$
\begin{aligned}
&P(\alpha \Uparrow_n,\beta \Uparrow_{n'}) = \\
&\quad\frac{1}{8}\Big\{2\Big(1-\cos(\vartheta-\vartheta')\cos\alpha\cos\beta\Big) \\
&\qquad+\Big\{2\sin(\vartheta-\vartheta')\Big(\cos\big(2\Delta\gamma(\vartheta)\big)\sin\alpha\cos\beta-\cos(2\Delta\gamma(\vartheta'))\cos\alpha\sin\beta\Big) \\
&\qquad\quad+\big(1-\cos(\vartheta-\vartheta')\big)\cos\big(2\Delta\gamma(\vartheta)+2\Delta\gamma(\vartheta')\big)\sin\alpha\sin\beta \\
&\qquad\quad-\big(1+\cos(\vartheta-\vartheta')\big)\cos\big(2\Delta\gamma(\vartheta)-2\Delta\gamma(\vartheta')\big)\sin\alpha\sin\beta\Big\}\Big\}
\end{aligned}
\tag{6.1.23}
$$

The same procedure can be done for the probability of finding on the left side spin up under an angle α from the quantization-axis $\vec{n}$ and on the right side to find spin down under an angle β from the quantization-axis $\vec{n}'$

$$
\begin{aligned}
P(\alpha \Uparrow_n, \beta \Downarrow_{n'}) = \Big\|\frac{1}{\sqrt{2}}\Big(&-a_1\, e^{2i(\gamma_+(\vartheta)+\gamma_+(\vartheta'))}\cos\frac{\alpha}{2}\sin\frac{\beta}{2} \\
&+a_2\, e^{2i(\gamma_-(\vartheta)+\gamma_-(\vartheta'))}\sin\frac{\alpha}{2}\cos\frac{\beta}{2} \\
&+a_3\, e^{2i(\gamma_+(\vartheta)+\gamma_-(\vartheta'))}\cos\frac{\alpha}{2}\cos\frac{\beta}{2} \\
&-a_4\, e^{2i(\gamma_-(\vartheta)+\gamma_+(\vartheta'))}\sin\frac{\alpha}{2}\sin\frac{\beta}{2}\Big)\Big\|^2
\end{aligned}
\tag{6.1.24}
$$

This gives the following general expression for the probability

$$
\begin{aligned}
&P(\alpha \Uparrow_n,\beta \Downarrow_{n'}) = \\
&\quad\frac{1}{8}\Big\{\Big(1-\cos\vartheta\cos\vartheta'-\sin\vartheta\sin\vartheta'\cos(\Delta\alpha_0)\Big)(1-\cos\alpha\cos\beta) \\
&\qquad+\Big(1+\cos\vartheta\cos\vartheta'+\sin\vartheta\sin\vartheta'\cos(\Delta\alpha_0)\Big)(1+\cos\alpha\cos\beta) \\
&\qquad-\Big\{(\cos(\Delta\alpha_0)(1-\cos\vartheta\cos\vartheta')-\sin\vartheta\sin\vartheta')\cos(2(\Delta\gamma(\vartheta)+\Delta\gamma(\vartheta')))\sin\alpha\sin\beta \\
&\qquad\quad+(-\cos(\Delta\alpha_0)\sin\vartheta\cos\vartheta'+\cos\vartheta\sin\vartheta')\cos(2(\Delta\gamma(\vartheta')))(1+\cos\alpha)\sin\beta \\
&\qquad\quad-(-\cos(\Delta\alpha_0)\cos\vartheta\sin\vartheta'+\sin\vartheta\cos\vartheta')\cos(2(\Delta\gamma(\vartheta)))\sin\alpha(1-\cos\beta) \\
&\qquad\quad-(\cos(\Delta\alpha_0)\cos\vartheta\sin\vartheta'-\sin\vartheta\cos\vartheta')\cos(2(\Delta\gamma(\vartheta)))\sin\alpha(1+\cos\beta) \\
&\qquad\quad+(\cos(\Delta\alpha_0)\sin\vartheta\cos\vartheta'-\cos\vartheta\sin\vartheta')\cos(2(\Delta\gamma(\vartheta')))(1-\cos\alpha)\sin\beta) \\
&\qquad\quad+(-\cos(\Delta\alpha_0)(1+\cos\vartheta\cos\vartheta')-\sin\vartheta\sin\vartheta')\cos(2(\Delta\gamma(\vartheta)-\Delta\gamma(\vartheta')))\sin\alpha\sin\beta\Big\}\Big\}
\end{aligned}
\tag{6.1.25}
$$

Again we set $\Delta\alpha_0 = 0$ and get

$$\begin{aligned}
&P(\alpha \Uparrow_n,\beta \Downarrow_{n'}) = \\
&\quad\frac{1}{8}\Big\{2\Big(1+\cos(\vartheta-\vartheta')\cos\alpha\cos\beta\Big) \\
&\qquad-\Big\{2\sin(\vartheta-\vartheta')\Big(\cos\big(2\Delta\gamma(\vartheta)\big)\sin\alpha\cos\beta-\cos(2\Delta\gamma(\vartheta'))\cos\alpha\sin\beta\Big) \\
&\qquad\quad+\big(1-\cos(\vartheta-\vartheta')\big)\cos\big(2\Delta\gamma(\vartheta)+2\Delta\gamma(\vartheta')\big)\sin\alpha\sin\beta \\
&\qquad\quad-\big(1+\cos(\vartheta-\vartheta')\big)\cos\big(2\Delta\gamma(\vartheta)-2\Delta\gamma(\vartheta')\big)\sin\alpha\sin\beta\Big\}\Big\}
\end{aligned} \tag{6.1.26}$$

Now we can calculate the expectation value[4]

$$\begin{aligned}
E(\alpha,\beta;n,n') =&2\big(P(\alpha \Uparrow_n,\beta \Uparrow_{n'})-P(\alpha \Uparrow_n,\beta \Downarrow_{n'})\big) \\
=&-\cos(\vartheta-\vartheta')\cos\alpha\cos\beta \\
&+\sin(\vartheta-\vartheta')\big(\cos\big(2\Delta\gamma(\vartheta)\big)\sin\alpha\cos\beta-\cos\big(2\Delta\gamma(\vartheta')\big)\cos\alpha\sin\beta\big) \\
&+\frac{1}{2}\Big(\big(1-\cos(\vartheta-\vartheta')\big)\cos\big(2\Delta\gamma(\vartheta)+2\Delta\gamma(\vartheta')\big) \\
&\quad-\big(1+\cos(\vartheta-\vartheta')\big)\cos\big(2\Delta\gamma(\vartheta)-2\Delta\gamma(\vartheta')\big)\Big)\sin\alpha\sin\beta
\end{aligned} \tag{6.1.27}$$

Bell inequality

We are going to consider the CHSH inequality, which is suitable to test such EPR entangled pairs in experiments. The CHSH inequality is given by the following combination of expectation values

$$\begin{aligned}
&S(\alpha,\beta,\gamma,\delta;n,n') = \\
&\qquad|E(\alpha,\beta;n,n')-E(\alpha,\gamma;n,n')|+|E(\delta,\beta;n,n')+E(\delta,\gamma;n,n')|\le 2
\end{aligned} \tag{6.1.28}$$

and has to be lower or even equal to two in a local realistic theory. When we insert the above calculated expectation value, equation (6.1.27), we get the following

[4] $\vartheta = \vartheta'$ gives the pure quantum mechanical expectation value.

expression

$$
\begin{aligned}
&S(\alpha,\beta,\gamma,\delta;n,n') = \\
&\quad = \Big| -\cos(\vartheta-\vartheta')\Big(\cos\alpha(\cos\beta-\cos\gamma)+\cos\delta(\cos\beta+\cos\gamma)\Big) \\
&\qquad + \sin(\vartheta-\vartheta')\Big\{\cos\big(2\Delta\gamma(\vartheta)\big)\Big(\sin\alpha(\cos\beta-\cos\gamma)+\sin\delta(\cos\beta+\cos\gamma)\Big) \\
&\qquad\qquad - \cos\big(2\Delta\gamma(\vartheta')\big)\Big(\cos\alpha(\sin\beta-\sin\gamma)+\cos\delta(\sin\beta+\sin\gamma)\Big)\Big\} \\
&\qquad + \frac{1}{2}\Big(\big(1-\cos(\vartheta-\vartheta')\big)\cos\big(2\Delta\gamma(\vartheta)+2\Delta\gamma(\vartheta')\big) \\
&\qquad\quad - \big(1+\cos(\vartheta-\vartheta')\big)\cos\big(2\Delta\gamma(\vartheta)-2\Delta\gamma(\vartheta')\big)\Big) \\
&\qquad\quad \Big(\sin\alpha(\sin\beta-\sin\gamma)+\sin\delta(\sin\beta+\sin\gamma)\Big)\Big|
\end{aligned}
\tag{6.1.29}
$$

This function is visualized in figure 6.3 for variable ϑ and ϑ' and fixed α, β, γ and δ, where we have taken the values $\alpha = 0$, $\beta = \frac{\pi}{4}$, $\gamma = \frac{3\pi}{4}$ and $\delta = \frac{\pi}{2}$. We see

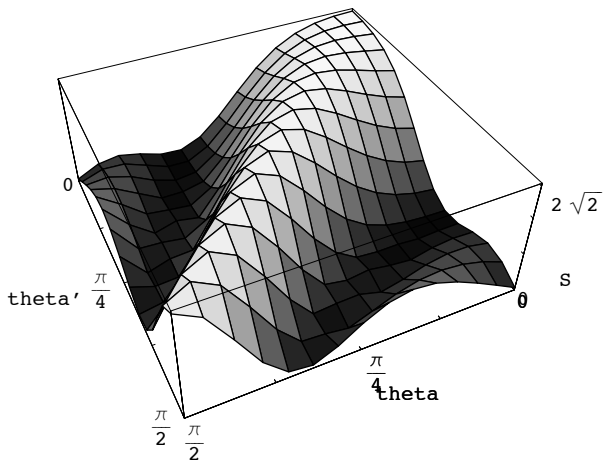

Figure 6.3: The S-function for ϑ and ϑ'.

clearly that also for the maximal violating angles of the pure quantum mechanic we reach values of S with appropriate values of ϑ and ϑ' that do not violate the CHSH inequality. That means we can find local realistic theories which describe the arising correlations. The function is symmetric in ϑ and ϑ' and reaches the maximum at $2\sqrt{2}$ for $\vartheta = \vartheta'$.

6.2 Quantum computer, quantum gates and Berry phase

6.2.1 Introduction

A **qubit** (=quantum bit) is the quantum mechanical analog of a classical bit. It is realized by a quantum system with two accessible orthogonal eigenstates represented by the two Boolean values $|0\rangle$ and $|1\rangle$. But in contrast to a classical bit this system can also exist in any superposition $\alpha|0\rangle + \beta|1\rangle$, where $|\alpha|^2+|\beta|^2= 1$. This is one of the reasons why quantum computers are more powerful than classical computers. Examples for qubits systems are atoms with two accessible energy levels, nuclear spins or polarized photons. A **quantum logic gate** is a device that performs a unitary operation on one qubit within a fixed period of time.

$$input \longrightarrow \boxed{\text{quantum logic gate}} \longrightarrow output$$

For a more extensive discussion of the basic features see for instance [22, 34].

Quantum logic gates

We can roughly distinguish between single qubit gates and two-qubit gates. For the single qubit gate case there are only two gates: the Hadamard gate H and the phase-shift gate Φ. In the two-qubit case we have the controlled phase shift gate $B(\phi)$ and the controlled-not (C-NOT) gate C. These four gates form a **universal set of gates**, which means we can built up any unitary transformation on qubits by using only these four gates. This is not a unique choice for a universal set of gates, but the most common one.
The **phase shift gate** ϕ acts on one qubit in the following way.

$$\begin{aligned} \Phi: \quad |0\rangle &\longrightarrow |0\rangle \\ |1\rangle &\longrightarrow e^{i\phi}|1\rangle \end{aligned}$$

This can be written in matrix form in the basis $\{|0\rangle, |1\rangle\}$ where we get

$$\Phi = \begin{pmatrix} 1 & 0 \\ 0 & e^{i\phi} \end{pmatrix} \tag{6.2.1}$$

The **Hadamard gate** H performs the following unitary transformation on the qubit

$$\begin{aligned} H: \quad |0\rangle &\longrightarrow \frac{1}{\sqrt{2}}(|0\rangle + |1\rangle) \\ |1\rangle &\longrightarrow \frac{1}{\sqrt{2}}(|0\rangle - |1\rangle) \end{aligned}$$

which gives in matrix form

$$H = \frac{1}{\sqrt{2}} \begin{pmatrix} 1 & 1 \\ 1 & -1 \end{pmatrix} \tag{6.2.2}$$

By combining a Hadamard gate and a phase shift gate one can produce arbitrary superpositions of $|0\rangle$ and $|1\rangle$.

The two-qubit gates consist of a control bit and a target bit. The **controlled phase shift gate** $B(\phi)$ is defined in such a way that the outcoming state gets a complex phase only if the control and the target bit are in the state $|1\rangle$. This reads in matrix form in the basis $\{|00\rangle, |01\rangle, |10\rangle, |11\rangle\}$ as

$$B(\phi) = \begin{pmatrix} 1 & 0 & 0 & 0 \\ 0 & 1 & 0 & 0 \\ 0 & 0 & 1 & 0 \\ 0 & 0 & 0 & e^{i\phi} \end{pmatrix} \tag{6.2.3}$$

The **C-NOT gate** C acts in the following way. When the control bit is in the state $|0\rangle$ nothing happens to the target bit but when the control bit is in the state $|1\rangle$ the target bit gets flipped. This can be expressed by the following matrix

$$C = \begin{pmatrix} 1 & 0 & 0 & 0 \\ 0 & 1 & 0 & 0 \\ 0 & 0 & 0 & 1 \\ 0 & 0 & 1 & 0 \end{pmatrix} \tag{6.2.4}$$

The C-NOT gate is very important because it allows to generate entangled states.

6.2.2 Realizations of quantum gates

There are many physical realizations of quantum computers and quantum gates (for a detailed discussion see for instance [52]). They all have to fulfill four basic requirements:

- There should be a distinct representation of the states $|0\rangle$ and $|1\rangle$.
- They should perform a controllable unitary evolution on the qubits.
- The desired input state should be prepared as the initial qubit state.
- The final state should be measurable to get the final qubit state.

These requirements can be achieved by several constructions. In the following we mention the most popular physical system with which quantum gates or quantum computation have been tried to realize yet.

Optical photon quantum computer Polarization states of the photon represents the two base states. Optical devices such as beam splitters, phase shifters and nonlinear Kerr media produce unitary operations. Preparation with laser light, detection via photomultiplier. But the nonlinear Kerr media used for the C-NOT produce too weak photon interactions.

Optical cavity quantum electrodynamics Single atoms are trapped into an optical cavity where they help the photons to interact with each other. For the remaining things the same principles as for the normal optical photon quantum computer are used.

Ion traps Ions are cooled in electromagnetic traps. The base states are represented by the hyperfine states of the atom, which can be manipulated by applying laser pulses. C-NOT gates can be realized by interaction of the ions via common phonons, which is difficult to prepare.

Nuclear magnetic resonance The spin of an atomic nucleus serves as the base states. They can be transformed by applying magnetic pulses to the spin in the strong magnetic field. Couplings are achieved by chemical bonds between neighboring atoms. The preparation and the measurement still causes some problems due to the reduced outgoing signal.

6.2.3 Geometric phases and NMR

Zanardi and Rasetti [81] were the first to point out that Berry phases could be used for enabling quantum computation. The idea was picked up [54], modified [53] and extended until the first experiments were done [41].

Geometric phases are proper candidates for realizing low noise quantum computing devices. Because of the dependence only on the net area traced out in phase space the geometric phase is an ideal construction for fault-tolerant quantum computation. The phase is achieved by nuclear magnetic resonance methods which already were used very early (1987,1988) to test Berry's phase in experiments [66, 67]. In the experiments a conditional geometric phase is applied, which means that the state of one spin determines the geometric phase acquired by the other spin. But the adiabatic geometric phase has also several drawbacks. First one is limited in time by the adiabatic condition which has to be removed to take full advantage of the short coherence time of the quantum computer. This can be done by using the more general concept of the Aharonov-Anandan phase (see for instance [74, 75, 76, 77]), which will not be discussed in this work. The second point is that one wants to get rid of the dynamical phase. This is done by using the so called spin-echo technique where the adiabatic evolution is applied twice in reversed direction. But here additional errors can be produced if the second path is not exactly the reversed of the first path and therefore the dynamical phase does not exactly cancel out.

Nuclear magnetic resonance

[5]We consider two qubit-gates therefore we start with a system consisting of two spins a and b in magnetic fields $\vec{B}_a$ and $\vec{B}_b$ along the z-axis. The Hamiltonian for this system is given by

$$H_0 = \frac{\hbar}{2}(\omega_a \, \sigma_{az} \otimes \mathbf{1}_b + \omega_b \, \mathbf{1}_a \otimes \sigma_{bz}) \tag{6.2.5}$$

where $\omega_a = \mu|\vec{B}_a|$ and $\omega_b = \mu|\vec{B}_b|$ denote the characteristic resonance frequencies of spin a, b and $\sigma_{az} = \sigma_{bz} = \sigma_z = \begin{pmatrix} 1 & 0 \\ 0 & -1 \end{pmatrix}$. This can be written in the basis of the

[5]This section follows references [33, 75, 77].

eigenstates (quantized along z-axis) of the Hamiltonian $\{|\Uparrow\Uparrow\rangle, |\Uparrow\Downarrow\rangle, |\Downarrow\Uparrow\rangle, |\Downarrow\Downarrow\rangle\}_{ab}$ in matrix form [6]

$$H_0 = \frac{\hbar}{2}\begin{pmatrix} \omega_a+\omega_b & 0 & 0 & 0 \\ 0 & \omega_a-\omega_b & 0 & 0 \\ 0 & 0 & -\omega_a+\omega_b & 0 \\ 0 & 0 & 0 & -\omega_a-\omega_b \end{pmatrix} \tag{6.2.6}$$

where we assume $\omega_a \neq \omega_b$ and $\omega_a > \omega_b$.

When we introduce interactions between the two spins the Hamiltonian H_0 modifies in the following way

$$\begin{aligned} H =& H_0 + \frac{\hbar}{2} J\ \sigma_{az} \otimes \sigma_{bz} \\ =& \frac{\hbar}{2}(\omega_a\ \sigma_{az} \otimes \mathbf{1}_b + \omega_b\ \mathbf{1}_a \otimes \sigma_{bz} + J\ \sigma_{az} \otimes \sigma_{bz}) \end{aligned} \tag{6.2.7}$$

where J denotes an interaction constant. This gives in matrix form

$$H = \frac{\hbar}{2}\begin{pmatrix} \omega_a+\omega_b+J & 0 & 0 & 0 \\ 0 & \omega_a-\omega_b-J & 0 & 0 \\ 0 & 0 & -\omega_a+\omega_b-J & 0 \\ 0 & 0 & 0 & -\omega_a-\omega_b+J \end{pmatrix} \tag{6.2.8}$$

Now we add a circularly polarized magnetic field $\vec{B}_x(t)$ in the xy-plane with the characteristic frequency $\omega_x = \mu|\vec{B}_x|$, a so called radio frequency (rf)-pulse and consider the Hamiltonian H'_a for spin a (trace out spin b). We get the following

$$H'_a = \frac{\hbar}{2}(\omega_a \pm J)\ \sigma_{az} + \frac{\hbar}{2}\omega_x\sigma_x(t) \tag{6.2.9}$$

where the $\pm$ sign in front of J depends on the specific state (up or down) of the spin b and $\sigma_x(t) = \begin{pmatrix} 0 & e^{-i\omega t} \\ e^{i\omega t} & 0 \end{pmatrix}$ with the angular frequency ω of the field $\vec{B}_x(t)$[7]. When we transform this Hamiltonian into the rotational frame for spin a rotating at speed ω we get

$$\begin{aligned} H_a =& RHR^{-1} + i(\frac{\partial}{\partial t}R)R^{-1} \\ =& \frac{\hbar}{2}(\omega_a - \omega \pm J)\sigma_z + \frac{\hbar}{2}\omega_x\sigma_x(t) \\ =& \frac{\hbar}{2}(\omega_\pm - \omega)\sigma_z + \frac{\hbar}{2}\omega_x\sigma_x(t) \end{aligned} \tag{6.2.10}$$

where $\omega_\pm = \omega_a \pm J$ and the rotational matrix is given by

$$R \equiv R(t) = e^{i\omega\frac{\sigma_z}{2}t} \tag{6.2.11}$$

[6] Tensor product: insert the second matrix into the first.

[7] Note that the field $\vec{B}_x(t)$ is described by two "frequencies". ω_x is the amplitude and ω the angular frequency of the field.

We see that for $|\omega_x| \ll |\omega_\pm - \omega|$ the Hamilton lies close to the z-axis and for $|\omega_x| \gg |\omega_\pm - \omega|$ it lies close to the x-axis. If the rf-pulse with frequency ω is applied in a way that we are far away from the resonance frequency $\omega_\pm$ then the system is quantized along the z-axis. If we are near resonance, $\omega = \omega_\pm$, then it is quantized along the x-axis. That means we can continuously sweep between both cases and furthermore if the variation is made adiabatically the spin of the system will follow the Hamiltonian. To acquire a Berry phase we want to obtain circular motions which can be imposed by adiabatically varying the phase of the rf-pulse. When the rf-pulse is not swept all the way to resonance but only to some final value ω_f we can implement cones with arbitrary opening angles ϑ (see figure 6.4).

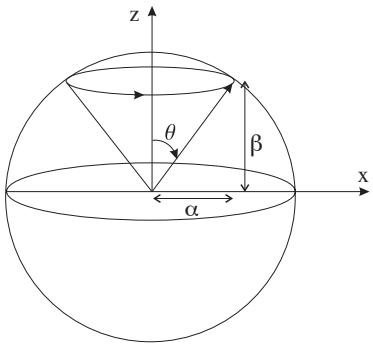

Figure 6.4: Setup for the geometrical phase in NMR: the frequencies $\alpha = \omega_x$ and $\beta = \omega_\pm - \omega$ are drawn in at the respective axes.

The opening angle is given by

$$\cos\vartheta_\pm = \frac{\omega_x}{\sqrt{(\omega_\pm - \omega)^2 + \omega_x^2}} \tag{6.2.12}$$

which gives for the Berry phase

$$\gamma_\pm = -\pi(1 - \cos\vartheta_\pm) \tag{6.2.13}$$

The Berry phase for spin a depends on the respective state of the spin b, we have applied a conditioned Berry phase. The next step is to remove the dynamical phase. This is done by a sequence of operations also known as spin echo approach. First the procedure to get a geometrical phase is applied to the system. Then the spin states are flipped by a short π pulse and the rotation due to the rf-pulse is repeated but in the other direction. Afterwards a π pulse is applied again to flip the states back to the original direction. After this procedure the system has acquired the following global phase factors written in matrix form

$$|\psi_f\rangle = \begin{pmatrix} e^{2i\Delta\gamma} & 0 & 0 & 0 \\ 0 & e^{-2i\Delta\gamma} & 0 & 0 \\ 0 & 0 & e^{-2i\Delta\gamma} & 0 \\ 0 & 0 & 0 & e^{2i\Delta\gamma} \end{pmatrix} |\psi_a\rangle \otimes |\psi_b\rangle \tag{6.2.14}$$

where $\Delta\gamma = \gamma_+ - \gamma_-$. This means the acquired geometric phase depends on the respective orientation of the two spins.

Experimental realization

The experimental realization of the theory explained above is due to Jones, Vedral, Ekert and Castagnoli [41]. They they used a sample consisting of 100 mg of 99% ^{13}C-labelled $CHCL_3$ dissolved in 0.2 ml of 99.96% $CDCl_3$. The ^{1}H nucleus are used as spin a and the ^{13}C as spin b. The interaction frequency between both nuclei is given by $J = 209.2$ Hz.

The frequency of the rf-pulse was set to $\omega_x = 221.3$ Hz and the frequency ω was varied between 0 and 774 Hz. The geometric phase was measured for both ^{1}H resonances. The results are shown in figure 6.5. We see clearly the splitting of the geometric phases due to the respective spin state.

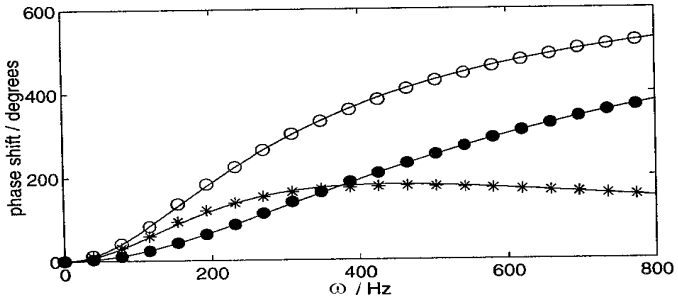

Figure 6.5: Experimental results for the conditional Berry phase with NMR: the filled circles show the results for γ_-, the open circles for γ_+ and the stars show $\Delta\gamma$. [41]

Chapter 7

Geometrical interpretation

7.1 Differential geometry

In this section we briefly want to discuss some basic features of the differential geometric language (see for instance [12, 50, 51]).

Differentiable manifold

A manifold M is a topological space ($dimM = n$) which locally looks like the Euclidian space $\mathbb{R}^n$. Globally it may have more complex structures. We can define so called charts $\{U_\alpha, \phi_\alpha\}$, that are homeomorphic maps ϕ_α form an open set $U_\alpha \subset M$ into an open set of $\mathbb{R}^n$. A manifold equipped with a differentiable structure is called a differentiable manifold.

Tangent space

A generalized definition of tangent vectors are differential operators over the manifold. The tangent vector $X = X^i \frac{\partial}{\partial x^i}$ is given by its action on a function $f(x^i(t))$ over M in local coordinates

$$Xf = \frac{d}{dt} f(x^i(t)) = \frac{d}{dt} x^i(t) \frac{\partial}{\partial x^i} f = X^i \frac{\partial}{\partial x^i} f \tag{7.1.1}$$

The X build up the a vector space, called tangent space $T_x(M)$ with the basis $\{\frac{\partial}{\partial x^i} \equiv \partial_i\}$.

Cotangent space

The dual space of $T_x(M)$ is the cotangent space $T_x^*(M)$. The basis $\{dx^i\}$ of the cotangent space is defined via the inner product

$$\left(dx^i, \partial_j\right) = \delta^i_j \tag{7.1.2}$$

In this space we can construct vectors, so called 1-forms $\omega = \omega_i dx^i$. They are defined by their action on a vector.

$$(\omega, X) = \left(\omega_i dx^i, X^j \partial_j\right) = \omega_i X^i \tag{7.1.3}$$

The concept of 1-forms can be extended to p-forms, also called differential forms. In general a p-form looks like

$$\omega = \frac{1}{p!}\omega_{\mu_1\mu_2\ldots\mu_p} dx^{\mu_1} \wedge dx^{\mu_2} \wedge \ldots \wedge dx^{\mu_p} \tag{7.1.4}$$

where the wedge product $\wedge$ is defined by an antisymmetric tensor product

$$dx^\mu \wedge dx^\nu = dx^\mu \otimes dx^\nu - dx^\nu \otimes dx^\mu \tag{7.1.5}$$

The set of all p-forms is a vector space denoted by Λ^p.

Exterior derivative

We can differentiate p-forms by introducing the exterior derivative d, which is a nilpotent ($d^2 = 0$) map

$$d : \Lambda^p \to \Lambda^{p+1} \tag{7.1.6}$$

in the following way

$$d\omega = \frac{1}{p!}\frac{\partial}{\partial x^\nu}\omega_{\mu_1\ldots\mu_p}(x)\; dx^\nu \wedge dx^{\mu_1} \wedge \ldots \wedge dx^{\mu_p} \tag{7.1.7}$$

Interior product

The interior product $\imath$ is a kind of generalized product that allows to multiply or contract a vector field X with a p-form ω. It is a map

$$\imath : \Lambda^p \to \Lambda^{p-1} \tag{7.1.8}$$

and defined in the following way

$$\imath_X \omega = \frac{1}{p!}\sum s = 1^p X^{\mu_s}\omega_{\mu_1\ldots\mu_s\ldots\mu_p}(-)^{s-1} dx^{\mu_1} \wedge \ldots \wedge \widehat{dx^{\mu_s}} \wedge \ldots \wedge dx^{\mu_p} \tag{7.1.9}$$

where the hat means that this term is left out. The interior product is nilpotent ($\imath^2 = 0$).

Hodge star operation

The Hodge star operation $*$ allows to transform an p-form ω_p into a (n-p)-form

$$* : \Lambda^p \to \Lambda^{n-p} \tag{7.1.10}$$

by the following action

$$*\omega_p = \frac{1}{p!(n-p)!}\omega_{\mu_1\ldots\mu_p}\varepsilon^{\mu_1\ldots\mu_p}{}_{\mu_{p+1}\ldots\mu_n} dx^{\mu_{p+1}} \wedge \ldots \wedge dx^{\mu_n} \tag{7.1.11}$$

The volume form $\varepsilon = \varepsilon_{\mu_1 \dots \mu_n} dx^{\mu_1} \wedge \dots \wedge dx^{\mu_n}$ is an n-form and the indices are raised or lowered by the metric tensor $g^{\mu\nu}$, therefore we have

$$\varepsilon^{\mu_1 \dots \mu_p}{}_{\mu_{p+1} \dots \mu_n} = g^{\mu_1 \nu_1} \cdots g^{\mu_p \nu_p} \varepsilon_{\nu_1 \dots \nu_p \mu_{p+1} \dots \mu_n} \tag{7.1.12}$$

When the Hodge star is applied twice we get the identity modulo a sign which is given by

$$** = \begin{cases} (-)^{p(n-p)} & \text{Euclidean} \\ (-)^{p(n-p)+1} & \text{Minkowskian} \end{cases} \tag{7.1.13}$$

Push forward map

We consider maps between two manifolds M and N. The smooth map $f : M \to N$ induces a map between the tangent spaces of the manifolds. This map is called the tangent map or push forward f_*

$$f_* : T_x(M) \to T_{f(x)}(N) \tag{7.1.14}$$

and is defined by its action on a vector field $X \in T_x(M)$

$$(f_* X)[g] = X[gf] \tag{7.1.15}$$

where $(f_* X) \in T_{f(x)}$, $g : N \to \mathbb{R}$ and $gf : M \to \mathbb{R}$. In figure 7.1 this has been visualized.

Pull back map

The map $f : M \to N$ induces also a map in the cotangent spaces, called the pull back map f^*

$$f^* : T^*_{f(x)}(N) \to T^*_x(M) \tag{7.1.16}$$

We note that the push forward f_* acts in the same direction as f but the pull back f^* acts in the opposite direction. f^* acts on a p-form ω in the following way

$$f^* \omega(X_1, \dots, X_p) = \omega(f_* X_1, \dots, f_* X_p) \tag{7.1.17}$$

For a visualization see again figure 7.1.

7.2 Fibre bundles

7.2.1 General setup

We are going to develop the concept of fibre bundles. A fibre bundle consists of the following ingredients.

- a topological space, the base space M
- a topological space, the total space E

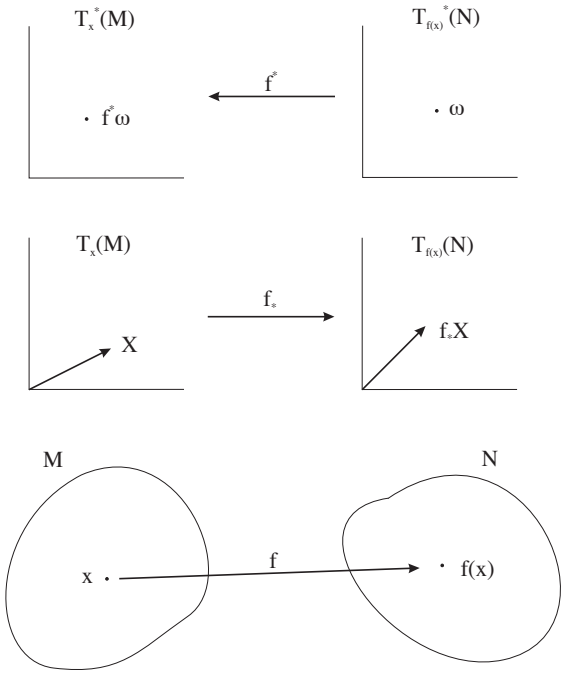

Figure 7.1: The action of the push forward map f_* and the pull back map f^*.

- a surjective map, the projection $\Pi : E \to M$
- a topological space, the standard fibre F with $\Pi^{-1}(x) = F_x \quad x \in M$
- a group, the structure group G

This is the setup for a general fibre bundle (E, Π, M, F, G) (see figure 7.2 . For our purpose the above mentioned topological spaces will be differentiable manifolds.

Globally a fibre bundle can have a complex structure (e.g. it can be twisted) but locally it has a simple product structure , which can be seen in the so called local trivialization. The base space M is covered by a set of open neighborhoods U_α, so called patches. For each U_α we can define a homeomorphism Φ_α in the following way:

$$\begin{aligned} &\forall\, U_\alpha \;\exists\, \Phi_\alpha : \Pi^{-1}(U_\alpha) \to U_\alpha \times F \\ &\text{such that} \quad \Pi\Phi_\alpha^{-1}(x, f) = x \qquad x \in U_\alpha \quad f \in F \end{aligned} \tag{7.2.1}$$

That means a local part $\Pi^{-1}(U_\alpha)$ of the bundle is mapped onto the direct product $U_\alpha \times F$ which is a simple untwisting of the bundle. The combination (U_α, Φ_α) denotes a set of local bundle coordinates. Under change of the local bundle coordinates from one patch U_α to another patch U_β, where the overlap $U_\alpha \cap U_\beta =: U_{\alpha\beta}$ is nonempty, we have to consider maps that have the form

$$g_{\alpha\beta} : U_{\alpha\beta} \times F \to U_{\alpha\beta} \times F \tag{7.2.2}$$

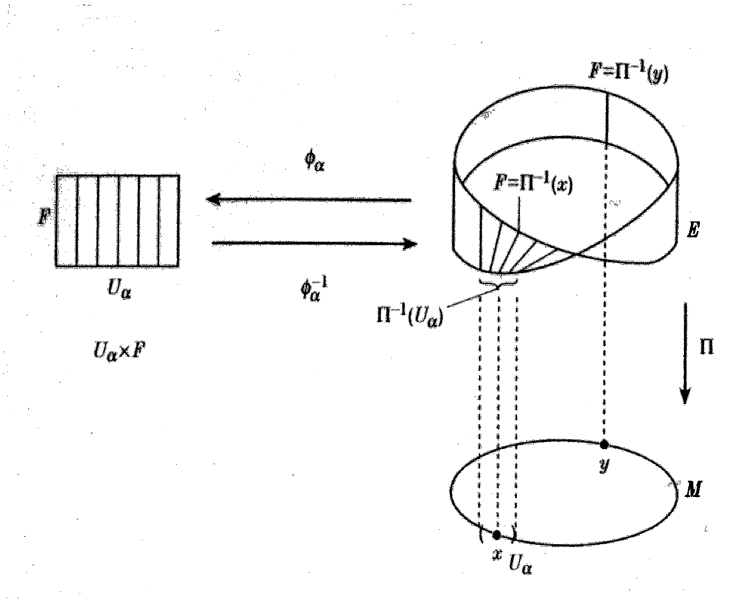

Figure 7.2: The simplest nontrivial example of a fibre bundle: the Möbius strip. [12]

These maps are called **transition functions**. It turns out that they are compositions of the homeomorphisms Φ_α

$$g_{\alpha\beta} = \Phi_\alpha \Phi_\beta^{-1} \tag{7.2.3}$$

and they form the structure group $G = \{g_{\alpha\beta}\}$. That means if we want to go from one fibre point f which belongs to the local trivialization (U_α, Φ_α) to another fibre point f' belonging to (U_β, Φ_β) this is done by left-action of the transition functions

$$f'(x) = g_{\beta\alpha}(x) \cdot f(x) \qquad x \in U_{\alpha\beta} \tag{7.2.4}$$

In a way the transition functions tell us how the fibres are glued together and therefore they give us the full information about the global structure of the bundle. There are two important properties. The first are the so called compatibility relations.

$$g_{\alpha\alpha}(x) = 1 \qquad x \in U_\alpha \tag{7.2.5}$$

$$g_{\alpha\beta}(x) = g_{\beta\alpha}^{-1}(x) \qquad x \in U_{\alpha\beta} \tag{7.2.6}$$

$$g_{\alpha\beta}(x) g_{\beta\gamma}(x) = g_{\alpha\gamma}(x) \qquad x \in U_{\alpha\beta\gamma} \tag{7.2.7}$$

The second concerns the uniqueness. That means there will be more than one set of transition functions defining the same bundle. They are transformed by an element of the structure group.

$$g'_{\alpha\beta}(x) = h_\alpha^{-1}(x) g_{\alpha\beta}(x) h_\beta(x) \qquad x \in U_{\alpha\beta} \tag{7.2.8}$$

If we speak in the following of a bundle we always mean an (topological) equivalence class of bundles.

A (global) **section** s of a bundle E is a continuous map with the following properties

$$s : M \to E \qquad \text{with} \quad \Pi(s(x)) = x \quad \forall x \in M \tag{7.2.9}$$

It is not always possible to define a global section of a bundle but it is possible to define local sections over open subsets of the base space M. The section transforms under change of the local coordinates via right-action of the transition functions

$$s_\beta(x) = s_\alpha(x) \cdot g_{\alpha\beta}(x) \qquad x \in U_{\alpha\beta} \tag{7.2.10}$$

Different kinds of fibre bundles:

Principal bundle: The fibre F_x is identical with the structure group G: $F_x \equiv G$. These bundles play an important role in physics.

Vector bundle: The fibre F_x is a vector space.

Line bundle: The fibre F_x is a one dimensional vector space, a line.

Associated bundle: The structure group has a certain representation ρ in a vector space. The transition functions of the associated bundle $h_{\alpha\beta}$ are now the images of transition functions of the original bundle $g_{\alpha\beta}$ under the representation of the group. $h_{\alpha\beta} = \rho(g_{\alpha\beta})$

Tangent bundle: The fibre F_x is the tangent space of the base manifold M: $F_x \equiv T_x(M)$

Cotangent bundle: The fibre F_x is the cotangent space of the base manifold M: $F_x \equiv T_x^*(M)$

7.2.2 Connection

We have seen, that we can reach different points on one fibre by multiplying them with an appropriate element of the structure group (see equation (7.2.4)). So we are able to move in a "vertical" direction. If we also want to move in the "horizontal" direction from one fibre to another we have to introduce the concept of the connection. This defines also how vectors are parallel transported. The following treatise will be based on principal bundles $P(M, G)$, where the structure group G is a Lie group and the base space M is a differentiable manifold.

For each fibre point $u \in P$ we can construct the tangent space $T_u(P)$. We can divide this tangent space into a vertical and a horizontal part (see figure 7.3. The vertical subspace $V_u(P)$ is defined in the following way, where X denotes a vector.

$$V_u(P) := \{X \in T_u(P) \mid \Pi_* X = 0\} \tag{7.2.11}$$

The horizontal subspace $H_u(P)$ is then given by the direct sum

$$T_u(P) = V_u(P) \oplus H_u(P) \tag{7.2.12}$$

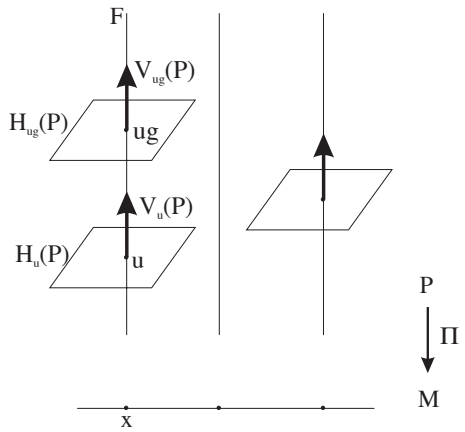

Figure 7.3: The decomposition of the tangent space $T_u(P)$ into vertical $V_u(P)$ and horizontal subspace $H_u(P)$.

Another way to define the horizontal subspace is done by the so called connection. A **connection** is a smooth function that defines for each fibre point u the horizontal subspace $H_u(P)$ in the following way

$$\begin{aligned} &\bullet\ T_u(P) = V_u(P) \oplus H_u(P) \text{ where } V_u(P) \text{ is defined by (7.2.11)} \\ &\bullet\ R_{g*}H_u(P) = H_{ug}(P) \end{aligned} \tag{7.2.13}$$

Here R_{g*} stands for the push forward of the right action $R_g u = ug$ of the structure group on the bundle. The second property defines how the subspaces of $H_u(P)$ and $H_{ug}(P)$ are related (see figure 7.3). This concept allows a clear decomposition of a tangent vector X into a vertical component X^V and a horizontal component X^H.

We want to consider now what happens when we try to lift up a tangent vector form the base space into the horizontal tangent space of the fibre. Given a tangent vector $X \in T_x(M)$ from the base manifold then we define the **horizontal lift** of this vector, denoted by $\tilde{X} \in H_u(P)$, in the following way

$$\begin{aligned} &\bullet\ \Pi_*\tilde{X} = X \quad \text{the projection of the lifted vector gives again the original vector} \\ &\bullet\ \tilde{X}^V = 0 \quad \text{the lifted vector has no vertical component} \end{aligned} \tag{7.2.14}$$

It is also possible to lift up curves in the same way. Given some curve $c : [0,1] \to M$ in the base manifold. The lifted curve $\tilde{c} : [0,1] \to P$ has to fulfill the following properties (see also figure 7.4)

$$\begin{aligned} &\bullet\ \Pi\tilde{c} = c \\ &\bullet\ \text{tangent vector to } \tilde{c}(t) \text{ is denoted by } \tilde{X}(t) \text{ and has no vertical component:} \\ &\quad \tilde{X}(t) \in H_{\tilde{c}(t)}(P) \text{ , that means all tangent vectors of } c \text{ are lifted into the} \\ &\quad \text{horizontal subspace} \end{aligned} \tag{7.2.15}$$

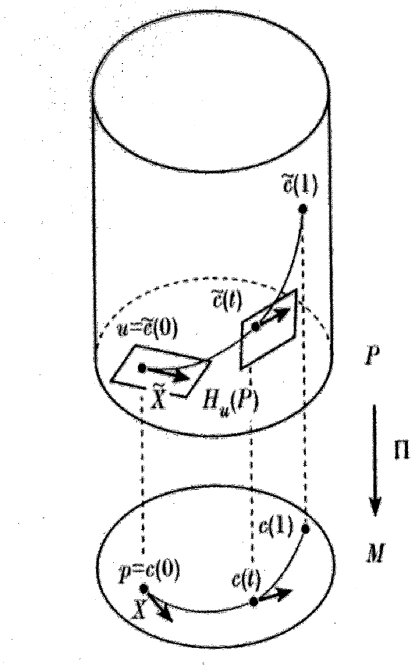

Figure 7.4: Horizontal lift of a curve c. [12]

If we have a curve c in the base space and we want to lift it in such a way that we specify the starting point in the bundle, that means $\tilde{c}(0) = u \in P$ then this determines the horizontal lift $\tilde{c}(t)$ uniquely for all t. Now let us assume that the curve c is closed. Does that automatically mean that the lifted curve is also closed? Obviously not. Such a phenomenon is called a **holonomy**. For a closed base curve c with $c(1) = c(0)$ in general the following property holds

$$\tilde{c}(1) = \tilde{c}(0)h \qquad \text{with } h \in G \tag{7.2.16}$$

The end- and the starting point differ by an element of the structure group. All possible elements h form again a group, the so called Holonomy group $H = \{h\}$, which is a subgroup of the structure group $H \subseteq G$.

Connection 1-form

In physics it is useful to work with the so called **connection 1-form** ω. This is a Lie algebra valued 1-form[1] on the bundle defined by the projection of the tangent space $T_u(P)$ onto the vertical subspace $V_u(P)$

$$\omega : T_u(P) \longrightarrow V_u(P) \tag{7.2.17}$$

The horizontal subspace is then defined as the kernel of the map ω

$$H_u(P) = \{X \in T_u(P) \mid \omega(X) = 0\} \tag{7.2.18}$$

[1]This is a 1-form tensored with an element of the Lie algebra.

This definition for the connection 1-form recovers the same properties as the definition for the connection therefore both concepts are equivalent.

In physics we are used to work in local coordinates. Therefore we have to find a representation of the connection 1-form. It turns out that locally the Yang-Mills gauge potential $\mathcal{A}$ assures all proposed properties and arises from pulling back the connection 1-form via a local section s_α to the base manifold M

$$\begin{aligned} s_\alpha : U_\alpha &\longrightarrow \Pi^{-1}(U_\alpha) \\ \mathcal{A}_\alpha &= s_\alpha^* \omega \end{aligned} \tag{7.2.19}$$

where $\{U_\alpha\}$ forms an open covering of M. The connection 1-form is uniquely defined on the bundle that means there is only one way of decomposing the tangent space into a horizontal and a vertical subspace. Therefore by choosing another patch in the above definition the respective connections must be equal

$$\omega \mid_{U_\alpha} \equiv \omega \mid_{U_\beta} \tag{7.2.20}$$

Then we get the following relation between the two resulting Yang-Mills potentials, which is valid in the overlap region $U_{\alpha\beta}$

$$\mathcal{A}_\beta = g_{\alpha\beta}^{-1} \mathcal{A}_\alpha g_{\alpha\beta} + g_{\alpha\beta}^{-1} d g_{\alpha\beta} \tag{7.2.21}$$

where $g_{\alpha\beta}$ are the transition functions from U_α to U_β and d denotes the exterior derivative on M. The above relation is called the **compatibility condition**, which the local Yang-Mills potential has to fulfill.

Curvature 2-form

First we have to define the **exterior covariant derivative** D on a p-form ϕ by

$$(D\phi)(X_1, \ldots, X_{p+1}) = (d_p \phi)(X_1^H, \ldots, X_{p+1}^H) \tag{7.2.22}$$

where the covariant derivative of the p-form is evaluated on $p+1$ vector fields X_i which lie in the tangent space of the bundle. This is equal to evaluating the exterior bundle derivative d_p of the p-form on the horizontal components of the vector fields.

The **curvature 2-form** Ω is defined as the covariant derivative of the connection 1-form.

$$\Omega = D\omega \tag{7.2.23}$$

The local representation of the curvature 2-form is given by the Yang-Mills field strength $\mathcal{F}$

$$\mathcal{F} = s^* \Omega \tag{7.2.24}$$

This can be written in terms of the Yang-Mills potential

$$\mathcal{F} = d\mathcal{A} + \mathcal{A}^2 \tag{7.2.25}$$

The compatibility condition of the field strength is given by

$$\mathcal{F}_\beta = g_{\alpha\beta}^{-1} \mathcal{F}_\alpha g_{\alpha\beta} \tag{7.2.26}$$

7.3 Geometric phase and geometry

7.3.1 Berry phase

The correspondence between fibre bundle and geometrical phase was first realized by Simon [64] in 1983[2], see also [4, 55]. We want to construct a fibre bundle that corresponds to the setup for Berry's phase. The base manifold M is equivalent to the parameter space $\{R\}$. At each point of the parameterspace the eigenstate of the system is defined up to a complex $U(1)$ phase by the eigenvalue equation (2.2.2). That means an eigenstate $|n\rangle$ is completely characterized by the pair $(R, e^{i\phi})$. This can be used to construct an associated line bundle to the principal fibre bundle with the structure group $G = U(1)$ and the fiber $F = U(1)$ (see figure 7.5). A section fixes the phase of the eigenstate in the bundle and corresponds to the selection of a physical state.

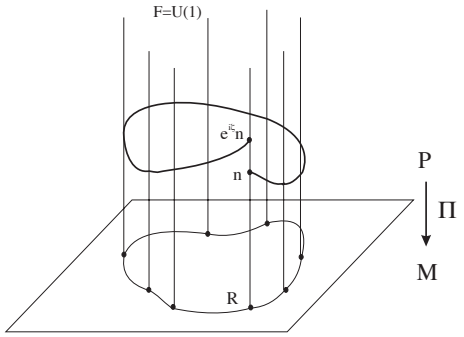

Figure 7.5: The fibre bundle for the Berry phase.

The time evolution of an eigenstate is represented by a curve in the bundle space P which corresponds to a curve in the base space M as the parameter R varies. As we have seen in the last section the way how the base curve is lifted to the bundle space is provided by the (local) connection 1-form[3]. In our special case of the adiabatic evolution this has to be a special sort of connection, the so called adiabatic connection. The local connection is given by the Yang-Mills gauge potential $\mathcal{A}$ which is in general defined as

$$\mathcal{A} = \sum_a A^a T^a \tag{7.3.1}$$

where $\{T^a\}$ denotes the generators of the Lie algebra. We have the $U(1)$ Lie group which gives only one generator for the Lie algebra $T^a = i$ for $a = 1$. Therefore we can identify the gauge potential $A_n(R)$ of equation (2.3.2) written as a differential form with the potential A^a, which gives

$$A^a \equiv A = A_n(R)dR = i\langle n|d|n\rangle \tag{7.3.2}$$

[2]It is interesting that his paper was published earlier (December 1983) than Berry's paper (March 1984).

[3]In the following we use the word connection rather than connection 1-form.

where d denotes the exterior derivative in the base space. Then the adiabatic connection is given by

$$\mathcal{A} = A^a T^a = iA = -\langle n|d|n\rangle \tag{7.3.3}$$

We can check the compatibility condition. We transform the fibre point $|n\rangle$ into another fibre point $|n'\rangle$ by left-multiplication with an element $g = e^{i\zeta}$ of the structure group $U(1)$

$$|n\rangle' = g \cdot |n\rangle = e^{i\zeta}|n\rangle \tag{7.3.4}$$

This corresponds to the gauge transformation of equation (2.3.3). Equation (7.2.21) then gives for the connection

$$\mathcal{A}' = \mathcal{A} - id\zeta \tag{7.3.5}$$

which is the gauge transformation law for the gauge potential. The last thing we want to do is to determine the holonomy group $\{e^{ih}\}$. This can be done by integrating the connection along a closed curve C

$$h = \oint_C \mathcal{A} = i \oint_C A = i\gamma(C) \tag{7.3.6}$$

We have used equation (2.3.1) to identify the holonomy with the Berry phase. We see that Berry's phase has a very natural interpretation as a holonomy in a fibre bundle.

Example: spin-$\frac{1}{2}$ particle in an adiabatically rotating magnetic field

When we apply the above construction to the spin-$\frac{1}{2}$ case, discussed in section 2.6, we get the following results. The connection is given by

$$\mathcal{A}_\pm = -\langle n|d|n\rangle = -\frac{i}{2}(1 \mp \cos\vartheta)\, d\phi \tag{7.3.7}$$

and we get for the holonomy

$$h = \oint_C \mathcal{A}_\pm = -i\pi(1 \mp \cos\vartheta) = i\gamma_\pm(C) \tag{7.3.8}$$

which recovers exactly the result for the Berry phase, given by equation (2.6.11)

$$\gamma_\pm(C) = -\pi(1 \mp \cos\vartheta) \tag{7.3.9}$$

7.3.2 Aharonov-Anandan phase

In the same way we can define a potential for the Aharonov-Anandan phase

$$\bar{A} = i\langle\xi|d|\xi\rangle \tag{7.3.10}$$

This defines the Aharonov-Anandan connection as

$$\bar{\mathcal{A}} = i\bar{A} = -\langle\xi|d|\xi\rangle \tag{7.3.11}$$

The gauge transformation

$$|\xi\rangle' = e^{i\zeta}|\xi\rangle \tag{7.3.12}$$

where $e^{i\zeta}$ is a $U(1)$ phase factor gives for the connection

$$\bar{\mathcal{A}}' = \bar{\mathcal{A}} - id\zeta \tag{7.3.13}$$

The holonomy which is the integral over a curve $\hat{C}$ is again related to the Aharonov-Anandan phase β

$$h = \oint_{\hat{C}} \bar{\mathcal{A}} = i \oint_{\hat{C}} \bar{A} = i\beta(\hat{C}) \tag{7.3.14}$$

Example: spin-$\frac{1}{2}$ particle in an arbitrary rotating magnetic field

The spin-$\frac{1}{2}$ case as discussed in section 3.4 gives us the following results. The Aharonov-Anandan connection is given by

$$\bar{\mathcal{A}}_\pm = -\frac{i}{2}(1 \mp \cos\bar{\vartheta})\, d\phi \tag{7.3.15}$$

which gives us for the holonomy

$$h = \oint_{\hat{C}} \bar{\mathcal{A}}_\pm = -i\pi(1 \mp \cos\bar{\vartheta}) = i\beta_\pm(\hat{C}) \tag{7.3.16}$$

This recovers exactly the result for the Aharonov-Anandan phase, given in equation (3.3.11)

$$\beta_\pm(\hat{C}) = -\pi(1 \mp \cos\bar{\vartheta}) \tag{7.3.17}$$

7.3.3 Generalized theory

We have seen that the Berry phase can be described with the help of the connection $\mathcal{A}$ of a complex line bundle L which is the associated $U(1)$ principal bundle over the parameterspace M

$$L \xrightarrow{\Pi} M \tag{7.3.18}$$

where the fibres L_R are given by the energy eigenrays of the Hilbertspace

$$L_R := \{c\,|n, R\rangle \;:\; c \in \mathbb{C}\} \tag{7.3.19}$$

The Aharonov-Anandan phase arises from the connection $\bar{\mathcal{A}}$ of the complex line bundle E which is again the associated $U(1)$ principal bundle but over the projective Hilbertspace $\mathcal{P}$

$$E \xrightarrow{\Pi} \mathcal{P} \tag{7.3.20}$$

Here the fibres are the rays of $\mathcal{P}$, that means for every state vector $|\eta\rangle$ lying in $\mathcal{P}$ the fibre is defined as

$$E_\xi := \{c\,|\xi\rangle \;:\; c \in \mathbb{C}\} \tag{7.3.21}$$

The two bundles are linked together (see figure 7.6) which can be described within the theory of the universal bundles. This is a rather complicated thing which we

are not going into deep here[4]. We just use one powerful statement: every special complex line bundle can be obtained as a pull back from the general bundle E. That means we can find a map f such that it maps between the two basis manifolds

$$f : M \longrightarrow \mathcal{P} \tag{7.3.22}$$

Than according to the above statement the bundle L is given by

$$L = f^*(E) \tag{7.3.23}$$

In our case the map f is given by

$$f(R) = |n, R\rangle\langle n, R| \tag{7.3.24}$$

The respective connection $\mathcal{A}$ of the bundle L can also be achieved by the pull back of the connection $\bar{\mathcal{A}}$

$$\mathcal{A} = f^*(\bar{\mathcal{A}}) \tag{7.3.25}$$

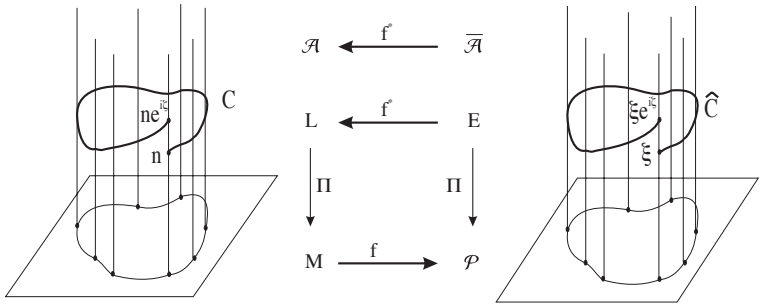

Figure 7.6: The relation between the Berry bundle and the Aharonov-Anandan bundle.

[4]For a more detailed discussion see for example [20, 48, 49].

List of Figures

Bibliography

[1] A.C. Aguiar-Pinto, M.C. Nemes, J.G. Peixoto de Faria, and M.T. Thomaz, "Comment on the adiabatic condition," *Am. J. Phys.* **68** (2000) 955–958, `quant-ph/9912030`.

[2] Y. Aharonov and J. Anandan, "Phase change during a cyclic quantum evolution," *Phys. Rev. Lett.* **58** (1987) 1593–1596.

[3] J. Anandan, J. Christian, and K. Wanelik, "Geometric phases in physics," *Am. J. Phys.* **65** (1997) 180–185.

[4] J. Anandan and L. Stodolsky, "Some geometrical considerations of Berry's phase," *Phys. Rev. D* **35** (1987) 2597–2600.

[5] J.S. Bell, "On the Einstein-Podolsky-Rosen paradox," *Physics* **1** (1964) 195–200.

[6] M.G. Benedict and L.G. Fehér, "Quantum jumps, geodesics, and the topological phase," *Phys. Rev. D* **39** (1989) 3194–3196.

[7] H.J. Bernstein and A.V. Phillips, "Fiber bundles and quantum theory," *Sci. Am.* **245** (1981) 94–109.

[8] M. V. Berry, "Quantal phase factors accompanying adiabatic changes," *Proc. R. Soc. Lond. A* **392** (1984) 45–57.

[9] M.V. Berry, "Quantum phase corrections from adiabatic iteration," *Proc. R. Soc. Lond. A* **414** (1987) 31–46.

[10] M.V. Berry, "Anticipations of the geometric phase," *Physics Today* (1990) 34–40.

[11] M.V. Berry, "Pancharatnam, virtuoso of the Poincaré sphere: an appreciation," *Curr. Sci.* **67** (1994) 220–223.

[12] R.A. Bertlmann, *Anomalies in Quantum Field Theory*. Oxford University Press, New York, 1996.

[13] R.A. Bertlmann, K. Durstberger, and B.C. Hiesmayr, "Berry phase for EPR-like entangled systems,". to be published.

[14] R.A. Bertlmann, W. Grimus, and B.C. Hiesmayr, "Bell inequality and CP violation in the neutral kaon system," *Phys. Lett. A* **289** (2001) 21–26, quant-ph/0107022.

[15] R.A. Bertlmann, W. Grimus, and B.C. Hiesmayr, *The EPR-paradox in massive systems or about strange particles.* [Un]Speakables of John Bell. R.A. Bertlmann and A. Zeilinger, 2002.

[16] R. Bhandari, "Observation of non-integrable geometric phase on the Poincaré sphere," *Phys. Lett. A* **133** (1988) 1–3.

[17] R. Bhandari and J. Samuel, "Observation of topological phase by use of a laser interferometer," *Phys. Rev. Lett.* **60** (1988) 1211–1213.

[18] T. Bitter and D. Dubbers, "Manifestation of Berry's topological phase in neutron spin rotation," *Phys. Rev. Lett.* **59** (1987) 251–254.

[19] A. Bohm, *Quantum Mechanics: Foundations and applications.* Springer-Verlag, New York, 1993.

[20] A. Bohm, L.J. Boya, A. Mostafazadeh, and G. Rudolph, "Classification theorem for principal fibre bundles, Berry's phase, and exact cyclic evolution," *J. Geometry and Physics* **12** (1993) 13–28.

[21] M. Born and V. Fock, "Beweis des Adiabatensatzes," *Z. Phys.* **51** (1928) 165–180.

[22] D. Bouwmeester, A. Ekert, and A. Zeilinger, *The physics of quantum information.* Springer-Verlag, Berlin, 2000.

[23] R.Y. Chiao, "Optical manifestation of Berry's topological phases: Aharonov-Bohm-like effects for the photon," *Proc. 3rd Int. Symp. Foundations of Quantum Mechanics, Tokyo* (1989) 80–92.

[24] R.Y. Chiao, A. Antaramian, K.M. Ganga, H. Jiao, S.R. Wilkinson, and H. Nathel, "Observation of a topological phase by means of a nonplanar Mach-Zehnder interferometer," *Phys. Rev. Lett.* **60** (1988) 1214–1217.

[25] R.Y. Chiao and Y.-S. Wu, "Manifestations of Berry's topological phase for the photon," *Phys. Rev. Lett.* **57** (1986) 933–936.

[26] T.H. Chyba, L.J. Wang, L. Mandel, and R. Simon, "Measurement of the Pancharatnam phase for a light beam," *Opt. Lett.* **13** (1988) 562–564.

[27] J.E. Clauser, M.A. Horne, A. Shimony, and R.A. Holt, "Proposed experiment to test local hidden-variable theories," *Phys. Rev. Lett.* **23** (1969) 880.

[28] G. Delacrétaz, E.R. Grant, R.L. Whetten, L. Wöste, and J.W. Zwanziger, "Fractional quantization of molecular pseudorotation in Na_3," *Phys. Rev. Lett.* **56** (1986) 2598–2601.

[29] D. Dubbers, "Nuclear reorientation in static and radio-frequency electro-magnetic fields," *Z. Phys. A* **276** (1976) 245–259.

[30] D. Dubbers, "Measurement of the Berry phase with polarized neutrons," *Physica B* **151** (1988) 93–95.

[31] P. Ehrenfest, "Adiabatische Invarianten und Quantentheorie," *Ann. d. Phys.* **51** (1916) 327.

[32] A. Einstein, B. Podolsky, and N. Rosen, "Can quantum-mechanical description of physical reality be considered complete?," *Phys. Rev.* **47** (1935) 777–780.

[33] A. Ekert, M. Ericsson, P. Hayden, H. Inamori, J.A. Jones, D.K.L. Oi, and V. Vedral, "Geometric quantum computer," `quant-ph/0004015`.

[34] A. Ekert, P. Hayden, and H. Inamori, "Basic concepts in quantum computation," `quant-ph/0011013`.

[35] J.C. Garrison and R.Y. Chiao, "Geometrical phases from global gauge invariance of nonlinear classical field theories," *Phys. Rev. Lett.* **60** (1988) 165–168.

[36] D.J. Griffiths, *Introduction to Quantum Mechanics*. Prentice-Hall, New Jersey, 1995.

[37] J.H. Hannay, "Angle variable holonomy in adiabatic excursion of an integrable Hamiltonian," *J. Phys. A: Math. Gen.* **18** (1985) 221–230.

[38] Y. Hasegawa, R. Loidl, M. Baron, G. Badurek, and H. Rauch, "Off-diagonal geometric phase in a neutron interferometer experiment," *Phys. Rev. Lett.* **87** (2001) 401–404.

[39] Y. Hasegawa, M. Zawisky, H. Rauch, and A.I. Ioffe, "Geometric phase in coupled neutron interference loops," *Phys. Rev. A* **53** (1996) 2486–2492.

[40] H. Jiao, S.R. Wilkinson, R.Y. Chiao, and H. Nathel, "Two topological phases in optics by means of a nonplanar Mach-Zehnder interferometer," *Phys. Rev. A* **39** (1989) 3475–3486.

[41] J.A. Jones, V. Vedral, A. Ekert, and G. Castagnoli, "Geometric quantum computation using nuclear magnetic resonance," *Nature* **403** (2000) 869–871, `quant-ph/9910052`.

[42] T. Kato, "On the adiabatic theorem of quantum mechanics," *J. Phys. Soc. Jpn.* **5** (1950) 435–439.

[43] P.G. Kwiat and R.Y. Chiao, "Observation of a nonclassical Berry's phase for the photon," *Phys. Rev. Lett.* **66** (1991) 588–591.

[44] E. Layton, Y. Huang, and S. Chu, "Cyclic quantum evolution and Aharonov-Anandan geometric phases in SU(2) spin-coherent states," *Phys. Rev. A* **41** (1990) 42–48.

[45] R. Leitgeb, *Geometric phases: connections and transport laws*. Diploma thesis, Technical University of Vienna, 1995.

[46] C.A. Mead and D.G. Truhlar, "On the determination of Born-Oppenheimer nuclear motion wave functions including complications due to conical intersections and identical nuclei," *J. Chem. Phys.* **70** (1979) 2284–2296.

[47] A. Messiah, *Quantenmechanik*, vol. 2. de Gruyter, Berlin, 1990.

[48] A. Mostafazadeh, "Geometric phase, bundle classification and group representation," *J. Math. Phys.* **37** (1996) 1218–1233, `hep-th/9312173`.

[49] A. Mostafazadeh and A. Bohm, "Topological aspects of the non-adiabatic Berry phase," `hep-th/9309060`.

[50] M. Nakahara, *Geometry, Topology and Physics*. Graduate student series in physics. Adam Hilger, Bristol, 1990.

[51] C. Nash and S. Sen, *Topology and Geometry for Physicists*. Academic Press, London, 1983.

[52] M.A. Nielsen and I.L. Chuang, *Quantum computation and quantum information*. Cambridge University Press, Cambridge, 2000.

[53] J. Pachos and S. Chountasis, "Optical holonomic quantum computer," *Phys. Rev. A* **62** (2000) 2318–2326, `quant-ph/9912093`.

[54] J. Pachos, P. Zanardi, and M. Rasetti, "Non-abelian Berry connections for quantum computation," *Phys. Rev. A* **61** (1999) 305–308, `quant-ph/9907103`.

[55] D.N. Page, "Geometrical description of Berry's phase," *Phys. Rev. A* **36** (1987) R 3479–3481.

[56] S. Pancharatnam, "Generalized theory of interference and its applications," *Proc. Indian Acad. Sci. A* **44** (1956) 247–262.

[57] S. Ramaseshan, "The Poincaré sphere and the Pancharatnam phase - some historical remarks," *Curr. Sci.* **59** (1990) 1154–1158.

[58] S. Ramaseshan and R. Nityananda, "The interference of polarized light as an early example of Berry's phase," *Curr. Sci.* **55** (1986) 1225–1226.

[59] D.J. Richardson, A.I. Kilvington, K. Green, and S.K. Lamoreaux, "Demonstration of Berry's phase using stored ultracold neutrons," *Phys. Rev. Lett.* **61** (1988) 2030–2033.

[60] C.W. Rupp, *Berry phase, Schwinger term, and anomalies in quantum field theory*. Diploma thesis, University of Vienna, 1998.

[61] J. Samuel and R. Bhandari, "General setting for Berry's phase," *Phys. Rev. Lett.* **60** (1988) 2339–2342.

[62] E. Schrödinger, "Die gegenwärtige Situation in der Quantenmechanik," *Naturwissenschaften* **23** (1935) 807;823;844.

[63] A. Shapere and F. Wilczek, *Geometric phases in physics*, vol. 5 of *Advanced Series in Mathematical Physics*. World Scientific, Singapore, 1989.

[64] B. Simon, "Holonomy, the quantum adiabatic theorem, and Berry's phase," *Phys. Rev. Lett.* **51** (1983) 2167–2170.

[65] R. Simon, H.J. Kimble, and E.C.G. Sudarshan, "Evolving geometric phase and its dynamical manifestation as a frequency shift: an optical experiment," *Phys. Rev. Lett.* **61** (1988) 19–22.

[66] D. Suter, G.C. Chingas, R.A. Harris, and A. Pines, "Berry's phase in magnetic resonance," *Mol. Phys.* **61** (1987) 1327–1340.

[67] D. Suter, K.T. Mueller, and A. Pines, "Study of the Aharonov-Anandan quantum phase by NMR interferometry," *Phys. Rev. Lett.* **60** (1988) 1218–1220.

[68] A. Tomita and R.Y. Chiao, "Observation of Berry's topological phase by use of an optical fiber," *Phys. Rev. Lett.* **57** (1986) 937–940.

[69] W.R. Tompkin, M.S. Malcuit, R.W. Boyd, and R.Y. Chiao, "Time reversal of Berry's phase by optical phase conjugation," *J. Opt. Soc. Am. B* **7** (1990) 230–233.

[70] R. Tycko, "Adiabatic rotational splittings and Berry's phase in nuclear quadrupole resonance," *Phys. Rev. Lett.* **58** (1987) 2281–2284.

[71] A.G. Wagh, G. Badurek, V.C. Rakhecha, R.J. Buchelt, and A. Schricker, "Neutron polarimetric separation of geometric and dynamical phases," *Phys. Lett. A* **268** (2000) 209–216.

[72] A.G. Wagh, V.C. Rakhecha, P. Fischer, and A. Ioffe, "Neutron interferometric observation of noncyclic phase," *Phys. Rev. Lett.* **81** (1998) 1992–1995.

[73] A.G. Wagh, V.C. Rakhecha, J. Summhammer, G. Badurek, H. Weinfurter, B.E. Allman, H. Kaiser, K. Hamacher, D.L. Jacobson, and S.A. Werner, "Experimental separation of geometric and dynamical phases using neutron interferometry," *Phys. Rev. Lett.* **78** (1997) 755–759.

[74] S.-J. Wang, "Nonadiabatic Berry's phase for a spin particle in a rotating magnetic field," *Phys. Rev. A* **42** (1990) 5107–5110.

[75] X.-B. Wang and M. Keiji, "NMR C-NOT gate through Aharonov-Anandan's phase shift," `quant-ph/0105024`.

[76] X.-B. Wang and M. Keiji, "Non-adiabatic conditional geometric phase shift with NMR," `quant-ph/0101038`.

[77] X.-B. Wang and M. Keiji, "On the nonadiabatic geometric quantum gates," `quant-ph/0108111`.

[78] C.L. Webb, R.M. Godun, G.S. Summy, M.K. Oberthaler, P.D. Featonby, C.J. Foot, and K. Burnett, "Measurement of Berry's phase using an atom interferometer," *Phys. Rev. A* **60** (1999) R 1783–1786.

[79] H. Weinfurter and G. Badurek, "Measurement of Berry's phase for noncyclic evolution," *Phys. Rev. Lett.* **64** (1990) 1318–1321.

[80] F. Wilczek and A. Zee, "Appearance of gauge structure in simple dynamical systems," *Phys. Rev. Lett.* **52** (1984) 2111–2114.

[81] P. Zanardi and M. Rasetti, "Holonomic quantum computation," *Phys. Lett. A* **264** (1999) 94, `quant-ph/9904011`.

[82] J.W. Zwanziger, M. Koenig, and A. Pines, "Berry's phase," *Annu. Rev. Phys. Chem.* (1990) 601–646.

Curriculum Vitae von Katharina Durstberger

Persönliche Daten:

Ich wurde am 16.06.1978 in Kirchdorf an der Krems (OÖ) als erstes Kind von Heinz und Christa Durstberger geboren.

Schulische Laufbahn:

1984-1988 Besuch der Volksschule in Roitham (OÖ)

1988-1996 Besuch des Realgymnasiums im Stift Lambach (OÖ) mit Schwerpunkt Darstellende Geometrie und Vertiefung in den Wahlpflichtfächern Mathematik und Informatik

Februar 1996 Verfassen einer Fachbereichsarbeit in Physik zum Thema "Die Theorie der Quarks unter besonderer Berücksichtigung der QCD" unter der Betreuung von Prof. Mag. Christian Kitzberger

Juni 1996 Matura mit ausgezeichnetem Erfolg bestanden

Oktober 1996 Beginn des Studiums der Physik und der Astronomie an der Universität Wien

Juli 1998 1. Diplomprüfung in Physik bestanden, 1. Diplomprüfung in Astronomie mit Auszeichung bestanden

September 2000 Besuch der Triangle Summer School in Praha (Tschechien)

Oktober 2000 Beginn der vorliegenden Diplomarbeit bei Prof. Dr. R. A. Bertlmann am Institut für Theoretische Physik der Universität Wien

10.-14. November 2000 Teilnahme an der Konferenz "Quantum [Un]speakables, conference in commemoration of John S. Bell"

September 2001 Besuch der Triangle Summer School in Modra (Slovakei)

September 2001 Teilnahme an der ÖPG-FAKT Tagung in Hollabrunn

Jänner 2002 Beendigung der Diplomarbeit und 2. Diplomprüfung in Physik